PTEP

Prog. Theor. Exp. Phys. **2023** 123B04(40 pages)
DOI: 10.1093/ptep/ptad147

The Petz (lite) recovery map for the scrambling channel

Yasuaki Nakayama[1,⋆], Akihiro Miyata [2,⋆], and Tomonori Ugajin[3,⋆]

[1]*Department of Physics, Kyoto University, Kitashirakawa, Kyoto 606-8502, Japan*
[2]*Kavli Institute for Theoretical Sciences, University of Chinese Academy of Sciences, Zhong-Guan-Cun East Road, Haidian District, Beijing 100190, China*
[3]*Department of Physics, Rikkyo University, Nishi-Ikebukuro, Toshima, Tokyo 171-8501, Japan*
⋆E-mail: nakayama@gauge.scphys.kyoto-u.ac.jp (Y.N.); akihiromiyata.physics@gmail.com (A.M.); ugajin@rikkyo.ac.jp (T.U.)

Received October 31, 2023; Revised December 4, 2023; Accepted December 6, 2023; Published December 7, 2023

We study properties of the Petz recovery map in chaotic systems, such as the Hayden–Preskill setup for evaporating black holes and the Sachdev–Ye–Kitaev (SYK) model. Since these systems exhibit the phenomenon called scrambling, we expect that the expression of the recovery channel $\mathcal{R}$ gets simplified, given by just the adjoint $\mathcal{N}^\dagger$ of the original channel $\mathcal{N}$ which defines the time evolution of the states in the code subspace embedded into the physical Hilbert space. We check this phenomenon in two examples. The first one is the Hayden–Preskill setup described by Haar random unitaries. We compute the relative entropy $S(\mathcal{R}[\mathcal{N}[\rho]]||\rho)$ and show that it vanishes when the decoupling is archived. We further show that the simplified recovery map is equivalent to the protocol proposed by Yoshida and Kitaev. The second example is the SYK model where the 2D code subspace is defined by an insertion of a fermionic operator, and the system is evolved by the SYK Hamiltonian. We check the recovery phenomenon by relating some matrix elements of an output density matrix $\langle T|\mathcal{R}[\mathcal{N}[\rho]]\,|T'\rangle$ to Rényi-two modular flowed correlators, and show that they coincide with the elements for the input density matrix with small error after twice the scrambling time.

Subject Index A61, B22, B30

1. Introduction

Advances in our understanding of the relationship between quantum information theory and holographic principles have revealed the connection between the structure of spacetime and quantum entanglement. In particular, the island formula [1–5] for the entropy of Hawking radiation implies that the island region in the interior of an old black hole is reconstructed from the information of Hawking radiation.

However, the precise way to recover a black hole interior region from Hawking radiation still remains to be understood. It has been realized that for this purpose, it is convenient to regard the black hole interior as a code subspace embedded in the Hilbert space of Hawking radiation as a quantum error correcting (QEC) code [6–8]. For instance, the decoupling theorem by Hayden and Preskill [6] implies that the black hole interior region is protected against the erasure of black hole degrees of freedom, which ensures the recovery. Once we regard an evaporating black hole as a QEC code, then the general argument of QEC [9] tells us that the recovery is achieved by applying the Petz recovery map [10,11].

Funded by SCOAP[3].

In this paper, we study properties of the Petz recovery map in chaotic systems, such as the Hayden–Preskill (HP) setup for evaporating black holes and the Sachdev–Ye–Kitaev (SYK) model. Since these systems exhibit the phenomenon called scrambling, we expect that the recovery channel $\mathcal{R}$ gets simplified, given by just the adjoint $\mathcal{N}^\dagger$ of the original channel $\mathcal{N}$ which defines the embedding of the black hole interior into the Hawking radiation. Therefore, schematically, we have

$$\mathcal{R} \sim a\,\mathcal{N}^\dagger, \tag{1}$$

where a is some numerical factor depending on the dimensions of the Hilbert spaces of black holes and Hawking radiation.

We will see this phenomenon in two examples. The first one is the HP setup where the dynamics of an evaporating black hole and Hawking radiation is described by Haar random unitaries. We do this by computing the relative entropy $S(\mathcal{R}\,[\mathcal{N}[\rho]]\,||\rho)$ and show that it is vanishing when the decoupling is archived. We further show that the simplified recovery map is equivalent to the Yoshida–Kitaev (YK) protocol.[1] The second example is one of the SYK model versions of the HP setup, discussed in Ref. [14].[2] In this setup, code information is expressed as excitations, and a system is evolved by the SYK Hamiltonian. We check the recovery phenomenon by relating some elements of an output density matrix $\langle T|\,\mathcal{R}[\mathcal{N}[\rho]]\,|T'\rangle$ to Rényi-two modular flowed correlators, and show that they give an input density matrix $\langle T|\,\rho\,|T'\rangle$ with small error after twice the scrambling time. However, there are still remaining matrix elements which we need to check, but it is difficult to evaluate them directly. In an upcoming paper [16], we will give their direct evaluations. In this paper, we do not evaluate them directly, but indirectly guess their expectations based on the result we obtained.

Our paper is organized as follows. In Sect. 2, we start with introducing a quantum channel induced by the HP setup, and explain how we write down the simplified recovery map in the original HP setup, which is applicable to the SYK case. We also explain a convenient notation to treat quantum channels induced by the HP setup, and in the notation, one can imagine gravitational interpretation simply. In Sect. 3, by using the convenient notation, we compute some relative entropies to check the condition of sufficiency that allows us to use the simplified recovery map as a recovery map. Also, we show that the YK protocol can be written as the recovery map. In Sect. 4, we explain one of the HP setups using the SYK model, and introduce a corresponding quantum channel. After that, we give the simplified recovery map, and show that some matrix elements of output results can be written as "Rényi-two modular flowed correlators." By evaluating the "Rényi-two modular flowed correlators" analytically, we show that some matrix elements of output results by the simplified recovery map give desired results. In Sect. 5, from the results we have computed in the previous section, we estimate the remaining matrix elements of output results which we are evaluating. The details of the remaining ones will be reported in an upcoming paper [16]. In Sect. 6, we conclude this paper with the discussion of our results and future directions. In Appendix A, we give another derivation of the simplified recovery map using a Kraus representation. In Appendix B, we show the relation that holds for an EPR state, which is used in Sect. 3. In Appendix C, conventions used in Sect. 4

[1] This equivalence has not been directly shown, but such an equivalence is suggested by Yoshida in Refs. [12,13].

[2] In Ref. [15], the authors discuss another HP setup in the SYK model, and the setup is different from our setup.

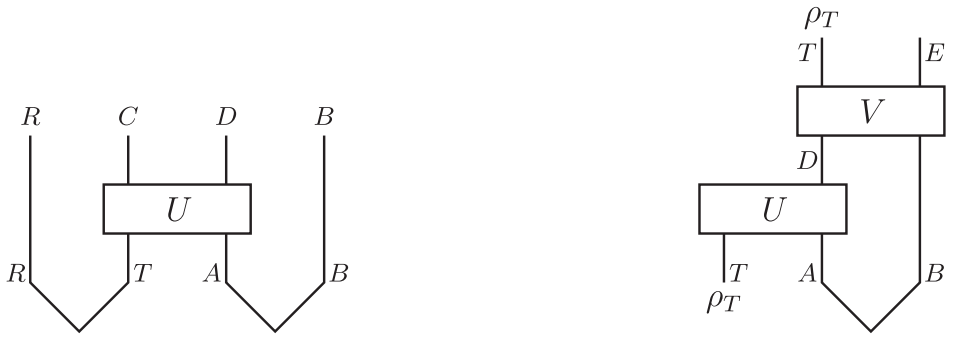

Fig. 1. Left: HP setup, corresponding to the state in Eq. (2). Right: Its decoder.

are listed. In Appendix D, we show that, in the SYK version of the HP setup, some recovery results can be written as "Rényi-two modular flowed correlators."

2. Recovery map for the HP channel

The HP setup is a tractable toy model for studying information flow in evaporating black holes. The setup consists of a black hole A that has been emitting Hawking radiation B. We are particularly interested in the system after the Page time where the black hole has emitted more than half of its original entropy,[3] therefore approximately forming a maximally entangled state $|\mathrm{EPR}\rangle_{AB}$. Suppose Alice throws a quantum state ρ_T (often called a diary) into this old black hole. Then, as the black hole further evaporates $A \to C + D$ by emitting late Hawking radiation D, information thrown into the black hole will eventually appear in total Hawking radiation DB. Here, we denoted by C the remaining black hole after emitting the late radiation D, see the left panel of Fig. 1. The analysis of Hayden and Preskill [6] showed that the diary appears in Hawking radiation almost immediately, namely after the scrambling time.

To see this, it is useful to introduce an additional system called reference R and form a maximally entangled state $|\mathrm{EPR}\rangle_{RT}$ with the diary T. Then, in this setup, the initial condition of the process is $|\mathrm{EPR}\rangle_{RT} \otimes |\mathrm{EPR}\rangle_{AB}$.

Owing to its chaotic dynamics, information of the diary thrown into the black hole gets scrambled and spreads over the entire degrees of freedom. The resulting state is given by

$$|\Psi_{\mathrm{HP}}\rangle = (I_R \otimes U_{T,A\to C,D} \otimes I_B)\, |\mathrm{EPR}\rangle_{R,T} \otimes |\mathrm{EPR}\rangle_{A,B}\,, \tag{2}$$

where I_R and I_B are identities in R and B, respectively, and $U_{T,\,A\,\to\,C,\,D}$ is a random unitary matrix from A, T to C, D, which models the chaotic dynamics of the black hole. By finding the Hilbert space with which R is mostly entangled, one can find where information of the original diary is in the final time slice. See again the left panel of Fig. 1.

The surprising result of HP is summarized in the following inequality:

$$\overline{\|\rho_{RC} - \rho_R \otimes \rho_C\|_1^2} \le \left(\frac{d_T}{d_D}\right)^2, \tag{3}$$

where $\|A\|_1 = \mathrm{tr}\sqrt{A^\dagger A}$, ρ_{RC}, ρ_R, ρ_C are the reduced density matrices of Eq. (2) on the indicated subsystems, d_D, d_T are the Hilbert space dimensions of subsystems D and T, respectively, and in the left-hand side we take an average over random unitaries. This inequality (3) implies that if one collects a sufficient number of late Hawking quanta so that $d_D \gg d_T$, the system of

[3] We follow the notation of YK [17].

the remaining black hole and the reference becomes no longer correlated $\rho_{RC} = \rho_R \otimes \rho_C$, and therefore the information of the diary has to be encoded in Hawking radiation DB.

This result is also natural from the viewpoint of the framework of quantum error correction.[4] A QEC code is a scheme to protect quantum states (logical states) in the code subspace H_{code} against various errors. Such an error is mathematically modeled by a completely positive and trace-preserving (CPTP) map called quantum channel $\mathcal{N}$. The basic idea of quantum error correction is protecting these quantum states in the code subspace H_{code} by embedding it into the larger Hilbert space, often called physical Hilbert space H_{phys}. In the HP protocol, the Hilbert space of the diary H_T corresponds to H_{code} in QEC, and H_{phys} is H_{DB}. The quantum channel $\mathcal{N} : T \to DB$ is obtained by tracing out the remaining black hole and the reference system degrees of freedom C and R from $|\Psi_{\text{HP}}\rangle$ in Eq. (2), by replacing the reference state $|\text{EPR}\rangle_{R,T}$ by $\sqrt{d_T \rho_T}\,|\text{EPR}\rangle_{R,T}$ (ρ_T is an input state),

$$\begin{aligned}\mathcal{N}_{T\to D,B}[\rho_T] &= \text{tr}_C\left[(U_{T,A\to C,D}\otimes I_B)(\rho_T \otimes |\text{EPR}\rangle_{A,B}\langle\text{EPR}|)(U^\dagger_{T,A\to C,D}\otimes I_B)\right] \\ &= \frac{1}{d_B}\sum_{\tilde{D},\tilde{D}'=1}^{d_D}\sum_{\tilde{B},\tilde{B}'=1}^{d_B} |\tilde{D}\rangle_D\langle\tilde{D}'| \otimes |\tilde{B}\rangle_B\langle\tilde{B}'| \sum_{C=1}^{d_C}\sum_{\tilde{T},\tilde{T}'=1}^{d_T} U_{C,\tilde{D};\tilde{T},\tilde{B}}(\rho_T)_{\tilde{T}\tilde{T}'}\, U^\dagger_{C,\tilde{D}';\tilde{T}',\tilde{B}'}.\end{aligned} \tag{4}$$

We call this quantum channel the HP channel.

Then, a general theorem of QEC[5] tells us that the decoupling condition is equivalent to the existence of a recovery map $\mathcal{R} : DB \to T$ which satisfies

$$\mathcal{R}[\mathcal{N}[\rho_T]] = \rho_T \quad \forall \rho_T \in H_T. \tag{5}$$

This again implies that the information of the diary is recoverable from Hawking radiation DB. See the right panel of Fig. 1. Moreover, the concrete expression of the recovery map is known [9], and is called the Petz recovery map:

$$\mathcal{R}^{\text{Petz}}_{\sigma,\mathcal{N}}[\tau] = \sigma^{\frac{1}{2}}\mathcal{N}^\dagger[(\mathcal{N}[\sigma])^{-\frac{1}{2}}\tau(\mathcal{N}[\sigma])^{-\frac{1}{2}}]\sigma^{\frac{1}{2}} \tag{6}$$

where σ is a full rank arbitrary density matrix on the code subspace H_{code}. The $\mathcal{N}^{-1/2}$ factor of the Petz recovery map is difficult to compute in general. One way of doing this is, as in Ref. [4], first making the replacement $\mathcal{N}^{-1/2} \to \mathcal{N}^n$, where n is a positive integer, computing it for all n, then taking analytic continuation $n \to -\frac{1}{2}$. Also, the $\mathcal{N}^{-1/2}$ part prevents us from obtaining the operational meaning of the map.

However, in systems exhibiting quantum chaos, we expect that the recovery map gets simplified, because $\mathcal{N}[\sigma]$ has a flat spectrum, therefore the approximation $\mathcal{R} \sim \mathcal{N}^\dagger$ appears to be possible.[6] If this is the case, since $\rho \sim \mathcal{N}^\dagger[\mathcal{N}[\rho]]$ for arbitrary density matrix ρ in the code subspace, therefore the relative entropy between them $S(\rho||\mathcal{N}^\dagger[\mathcal{N}[\rho]])$ vanishes.

[4] We note that the possible maximum number of late Hawking radiation d_D is given by the input for the Haar random unitary, implying $d_D \le d_T d_B$. Due to this bound, the combination d_T/d_D cannot be 0, but at most $1/d_B$. Thus, the exact equality does not hold $\rho_{RC} = \rho_R \otimes \rho_C$, as long as d_B is finite. This means that, strictly speaking, the recovery of the diary from Hawking radiation is, at best, approximate. However, for a sufficiently large dimension of the early radiation, $d_B \gg 1$, we can almost ignore the deviation from the exact factorization of ρ_{RC} for late times.

[5] See, e.g. Refs. [18,19] for the theorem.

[6] In Appendix A, we give another equivalent argument supporting our expectation of this simplification in terms of the Kraus representation of the HP channel.

For the HP channel, the adjoint HP channel $\mathcal{N}^\dagger$ is given by

$$\begin{aligned}\mathcal{N}^\dagger_{D,B\to T}[\mathcal{O}_{DB}] &= \mathrm{tr}_{A,B}\left[|\mathrm{EPR}\rangle_{A,B}\langle\mathrm{EPR}|\,(U^\dagger_{T,A\to C,D}\,\mathcal{O}_{DB}\,U_{T,A\to C,D})\right]\\ &= {}_{A,B}\langle\mathrm{TFD}|\left(U^\dagger_{T,A\to C,D}\otimes I_B\right)(\mathcal{O}_{DB}\otimes I_C)\,(U_{T,A\to C,D}\otimes I_B)\,|\mathrm{TFD}\rangle_{A,B}\,.\end{aligned} \tag{7}$$

Here, the adjoint channel is defined by the relation[7]

$$\mathrm{tr}_{D,B}\left[\mathcal{N}_{T\to D,B}[\rho_T]\;O_{DB}\right] = \mathrm{tr}_T\left[\rho_T\,\mathcal{N}^\dagger_{D,B\to T}[\mathcal{O}_{DB}]\right]. \tag{9}$$

For later convenience, we introduce a correctly normalized recovery map

$$\mathcal{R}^{\mathrm{Lite}}_{D,B\to T}[\mathcal{O}_{DB}] \coloneqq \frac{1}{N}\cdot\frac{d_B d_D}{d_T}\mathcal{N}^\dagger_{D,B\to T}\left[\mathcal{O}_{DB}\right], \tag{10}$$

and define it as the *Petz-lite*.[8] Here, N is the normalization constant

$$N = \left(\frac{d_D}{d_T}\right)^2 + 1, \tag{11}$$

determined by the condition $\overline{\mathrm{tr}_T\left[\mathcal{R}^{\mathrm{Lite}}_{D,B\to T}\left[\mathcal{N}_{T\to D,B}[\sigma_T]\right]\right]} = 1$, where σ_T is some reference state in T. In the Haar random case, the choice of the reference state σ_T is not important as long as it is normalized.

With this N, the Petz-lite can be expressed as

$$\begin{aligned}\mathcal{R}^{\mathrm{Lite}}_{D,B\to T}[\mathcal{O}_{DB}] &= \frac{1}{\left(\frac{d_D}{d_T}\right)^2+1}\cdot\frac{d_B d_D}{d_T}\mathcal{N}^\dagger_{D,B\to T}\left[\mathcal{O}_{DB}\right]\\ &= \frac{1}{1+\left(\frac{d_T}{d_D}\right)^2}\cdot d_C\,\mathcal{N}^\dagger_{D,B\to T}\left[\mathcal{O}_{DB}\right],\end{aligned} \tag{12}$$

where in the second line, we used the relation $d_B d_T = d_C d_D$ due to the unitarity of the Haar random unitary. For the parameter region $d_T/d_D \ll 1$, the normalization is just given by d_C, which coincides with an expression obtained from another discussion. In Appendix A, we give the discussion.

2.1. *West-coast notation and replica-wormhole-like objects*

In the following, we are interested in the typical properties of the recovery map $\mathcal{R}$ for the HP channel $\mathcal{N}$. To investigate these properties, we will consider replicated quantities, such as $\mathrm{tr}(\mathcal{N}[\rho_T])^n$ involving a product of Haar random unitaries and its average. Since such averaging involves Wick-type contractions between various pairs of Haar random unitaries in the product, it is convenient to introduce a graphical notation that manifests which pair of unitaries are contracted. Therefore, here we introduce a notation similar to the one employed in Ref. [4]

[7] More generally, for a quantum channel $\mathcal{N}$, its adjoint channel is defined by the similar relation,

$$\mathrm{tr}\left[\mathcal{N}\left[\rho\right]O\right] = \mathrm{tr}\left[\rho\,\mathcal{N}^\dagger\left[O\right]\right]. \tag{8}$$

[8] The terminology "Petz-lite" is introduced in Ref. [4], and we also use this terminology in this paper.

for modeling the black hole microstates and their statistical properties, and call this West-coast notation.

To begin with, let us define the following black hole microstate on C, involving a Haar random unitary:

$$\left|\psi_i^T\right\rangle_C \coloneqq \sqrt{d_C\, d_D}\sum_{C=1}^{d_C} |C\rangle\, U_{C,T;i}. \tag{13}$$

Here, $\{|C\rangle\}$ is the set of basis states on the Hilbert space H_C and the index i collectively denotes the indices for both late radiation D and early radiation B, i: (D, B), or more concretely $|i\rangle = |D\rangle \otimes |B\rangle$, thus the label i runs from 1 to $d_D d_B \equiv k$.

In the following, we use this type of states $\left|\psi_i^T\right\rangle_C$ to write quantities of our interest, instead of random unitary matrices $U_{C,\,D;\,T,\,B}$. Under this notation, we can write

$$\left\langle \psi_i^T \middle| \psi_j^{T'} \right\rangle = d_C\, d_D \sum_{C=1}^{d_C} U^\dagger_{i;C,T}\, U_{C,T';j} \tag{14}$$

and therefore the HP channel (4) is given by

$$\mathcal{N}_{T\to D,B}[\rho_T] = \frac{1}{k d_C}\sum_{i,j=1}^{k} |i\rangle\langle j| \cdot \sum_{\tilde{T},\tilde{T}'=1}^{d_T} \left\langle \psi_j^{\tilde{T}'} \middle| \psi_i^{\tilde{T}} \right\rangle (\rho_T)_{\tilde{T}\tilde{T}'}. \tag{15}$$

In this notation, we call the subscript index i Hawking radiation index, and the superscript T code index.

The West-coast model treats each of these microstates $|\psi_i\rangle$ by a single-sided anti-de Sitter (AdS) black hole with insertion of an "end of the world brane" (or EoW brane in short) labeled by the index i behind the horizon. This state has a Hartle–Hawking-type preparation, in terms of a Euclidean path integral with the EoW brane which starts from the Euclidean conformal boundary. In this model, the overlap between two such states $\langle\psi_i|\psi_j\rangle$ is computed by a Euclidean gravitational path integral on a region of Euclidean disc enclosed by the part of the asymptotic boundary (an interval) and the EoW brane in the bulk.

With this gravitational path integral picture in mind, here we explain the fact that there is a simple diagrammatic prescription to compute a product of such overlaps $\overline{\prod_{m=1}^n \langle\psi_{i_m}^{a_m}|\psi_{j_m}^{b_m}\rangle}$[9] without directly applying the formulae for the Haar random averages, which becomes quite involved when the number of unitary matrices appearing increases.

Then the prescription is the following:

(1) For each overlap in the product $\langle\psi_{i_m}^{a_m}|\psi_{j_m}^{b_m}\rangle$ draw an interval with two endpoints, and associate the labels (i_m, a_m) to one end and (j_m, b_m) to the other. (In the West-coast model, this interval with indices at the endpoints provides the boundary condition to the gravitational path integral for the product of the overlaps.)

(2) The n intervals prepared in this way have $2n$ endpoints in total. We pick up two of these endpoints and connect them by a line, which we call the EoW brane. We repeat this until all the endpoints are connected to the other by EoW branes. There are many different ways to do this. One possibility is that the endpoint of the m-th interval is always

[9] In the West-coast paper, this quantity is just called the product of overlap and denoted without the bar, i.e. $\overline{\prod_{m=1}^n \langle\psi_{i_m}^{a_m}|\psi_{j_m}^{b_m}\rangle}\Big|_{\text{ours}} = \prod_{m=1}^n \langle\psi_{i_m}^{a_m}|\psi_{j_m}^{b_m}\rangle_{\text{WC}}$. We will use the convention with the bar to keep in mind that we do average over random unitaries in the computation.

connected to the other endpoint of the same interval. Or another possibility is that the endpoint of the m-th interval is always connected to the point on the next $(m+1)$-th interval.

(3) Each diagram D constructed in this way contains n EoW branes. We then associate each EoW brane in the diagram with a Kronecker delta factor. If the EoW brane is connecting two endpoints with the labels (i_l, a_l) and (j_m, b_m), then this factor is given by $\delta_{i_l j_m}\delta_{a_l b_m}$. We compute this for all EoW branes in the diagram and then multiply these factors. Let us denote this factor for the diagram by I_D.

(4) Since each diagram can be regarded as (a disjoint union of) 2D surfaces, we can associate an Euler number χ_D to the diagram. We then pick up the factor $(d_C)^{\chi_D}$ which corresponds to the gravitational path integral part in the West-coast model. We then sum the total factor $I_D(d_C)^{\chi_D}$ for all possible diagrams D.

(5) The average of the overlaps is equal to the sum of these factors over all possible diagrams:

$$\overline{\prod_{m=1}^{n}\left\langle \psi_{i_m}^{a_m}|\psi_{j_m}^{b_m}\right\rangle} = \sum_{D\in\text{All diagrams}} I_D\,(d_C)^{\chi_D}. \tag{16}$$

Let us provide a few examples. First, for the single overlap $\overline{\left\langle \psi_i^T\middle|\psi_j^{T'}\right\rangle}$. We can easily evaluate it:

$$\begin{aligned}\overline{\left\langle \psi_i^T\middle|\psi_j^{T'}\right\rangle} &= d_C\,d_D\sum_{C=1}^{d_C}\overline{U^\dagger_{i;C,T}\,U_{C,T';j}}\\ &= d_C\,\underbrace{\delta_{D_iD_j}\,\delta_{B_iB_j}}_{\delta_{ij}}\,\delta_{TT'}\\ &= d_C\,\delta_{ij}\,\delta_{TT'},\end{aligned} \tag{17}$$

where in the second line, we used the general result for two Haar random unitaries

$$\overline{U_{a,b}U^\dagger_{c,d}} = \frac{1}{d}\,\delta_{ad}\delta_{bc} \qquad (a,b,c,d=1,\cdots,d). \tag{18}$$

This result can be easily reproduced from the West-coast prescription.

Next, let us evaluate the Haar average of the combination of the overlaps for later convenience,

$$\left\langle \psi_i^{T_1}\middle|\psi_j^{T_1'}\right\rangle\cdot\left\langle \psi_j^{T_2'}\middle|\psi_i^{T_2}\right\rangle. \tag{19}$$

Clearly, by setting $T_1 = T_2 = T$ and $T_1' = T_2' = T'$, the above combination reduces to the variance of the overlap $\overline{\left|\left\langle \psi_i^T\middle|\psi_j^{T'}\right\rangle\right|^2}$. We can evaluate the above quantity by the diagrammatic prescription mentioned above (see Fig. 2),

$$\overline{\left\langle \psi_i^{T_1}\middle|\psi_j^{T_1'}\right\rangle\cdot\left\langle \psi_j^{T_2'}\middle|\psi_i^{T_2}\right\rangle} \approx (d_C)^2\,\delta_{ij}\delta_{T_1T_1'}\cdot\delta_{ji}\delta_{T_2'T_2} + d_C\,\delta_{ii}\delta_{T_1T_2}\cdot\delta_{jj}\delta_{T_2'T_1'}. \tag{20}$$

Fig. 2. Diagrams for computing the average of overlaps (20). A black line connects two points that appear in the same overlap, and the blue lines correspond to the EoW branes in Haar random averaging. Left: The disconnected diagram. Right: The connected diagram.

This coincides with the result obtained by using the Weingarten formula,

$$\overline{U_{a_1,b_1}U^\dagger_{c_1,d_1}\cdot U_{a_2,b_2}U^\dagger_{c_2,d_2}} = \frac{1}{d^2-1}\left(\delta_{a_1d_1}\delta_{b_1c_1}\cdot\delta_{a_2d_2}\delta_{b_2c_2}+\delta_{a_1d_2}\delta_{b_1c_2}\cdot\delta_{a_2d_1}\delta_{b_2c_1}\right)$$
$$+\frac{1}{d\left(d^2-1\right)}\left(\delta_{a_1d_1}\delta_{a_2d_2}\delta_{b_1c_2}\delta_{b_2c_1}+\delta_{a_1d_2}\delta_{a_2d_1}\delta_{b_1c_1}\delta_{b_2c_2}\right)$$
$$\times\,(a,b,c,d=1,\cdots,d). \tag{21}$$

In general, the prescription introduced here correctly computes the average over Haar random unitaries in the product of overlaps, as long as the rank of the random unitaries $d = d_C\,d_D = d_T\,d_A$ is large.

Furthermore, the adjoint channel (7), in terms of the West-coast notation, is given by

$$\mathcal{N}^\dagger_{D,B\to T}[\mathcal{O}_{DB}] = \frac{1}{kd_C}\sum_{T,T'=1}^{d_T}|T'\rangle\langle T|\cdot\sum_{i,j=1}^{k}\left\langle\psi_j^{T'}\middle|\psi_i^{T}\right\rangle\langle j|\,\mathcal{O}_{DB}\,|i\rangle\,. \tag{22}$$

Below, using this graphical expression, we evaluate several relative entropies to check the validity of the approximation $\mathcal{R}\sim\mathcal{N}^\dagger$.

3. Relative entropy: sufficiency

As we have mentioned, the decoupling condition (3) implies that there is a recovery map for the HP channel (4). Another characterization of the existence of the recovery map $\mathcal{R}$ for given $\mathcal{N}$ is the notion of sufficiency [10,11,20]. To state this, let us first recall the fact that relative entropy satisfies the monotonicity property

$$S(\rho||\sigma)\geq S(\mathcal{N}[\rho]||\mathcal{N}[\sigma]) \tag{23}$$

for any CPTP map $\mathcal{N}$. By repeating this, we have

$$S(\rho||\sigma)\geq S(\mathcal{N}[\rho]||\mathcal{N}[\sigma])\geq S(\mathcal{R}[\mathcal{N}[\rho]]||\mathcal{R}[\mathcal{N}[\sigma]]), \tag{24}$$

therefore, if the recovery map exists $\mathcal{R}\circ\mathcal{N}=1_{\rm code}$, then $S(\rho||\sigma)=S(\mathcal{N}[\rho]||\mathcal{N}[\sigma])$, for any density matrices on the code subspace. This condition is known as sufficiency, and it was shown that if $\mathcal{N}$ satisfies this condition, the recovery map is given by Eq. (6). Here we would like to check the HP channel (4) does satisfy sufficiency, by directly computing the relative entropy $S(\mathcal{N}[\rho]||\mathcal{N}[\sigma])$ in the presence of the quantum channel $\mathcal{N}$.[10]

Since our interest is a typical result under the Haar random average, we consider the Haar averaged relative entropy, $\overline{S(\mathcal{N}[\rho]||\mathcal{N}[\sigma])}$. To evaluate the relative entropy, we use the replica trick [23]:

$$\overline{S(\mathcal{N}[\rho]||\mathcal{N}[\sigma])}=\lim_{n\to1}\frac{1}{n-1}\left(\overline{\log\mathrm{tr}\left[\mathcal{N}[\rho]^n\right]}-\overline{\log\mathrm{tr}\left[\mathcal{N}[\rho]\mathcal{N}[\sigma]^{n-1}\right]}\right). \tag{25}$$

[10] See Refs. [21,22] for related discussions on original Petz map cases.

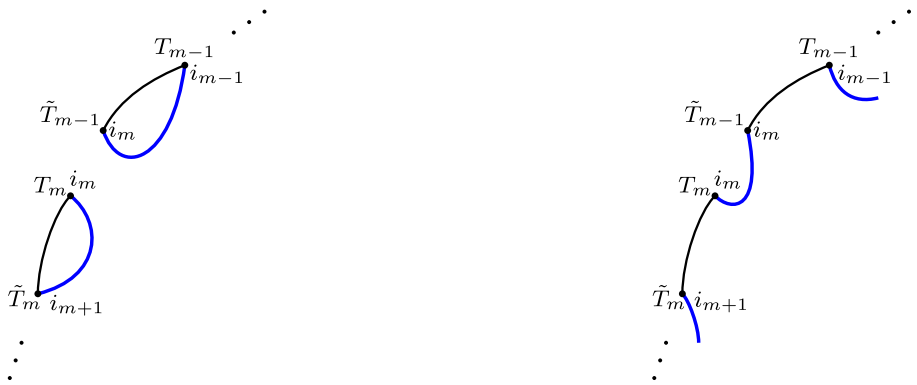

Fig. 3. Left: The dominant diagram for Eq. (27) when $d_D \ll d_T$ (disconnected diagram). Right: The connected diagram dominating the sum at $d_T \ll d_D$.

Generally, since it is difficult to evaluate the Haar average of logarithmic functionals, instead of the expression, we consider

$$\overline{S(\mathcal{N}[\rho]||\mathcal{N}[\sigma])} \approx \lim_{n\to 1} \frac{1}{n-1}\left(\log \overline{\mathrm{tr}\,[\mathcal{N}[\rho]^n]} - \log \overline{\mathrm{tr}\left[\mathcal{N}[\rho]\mathcal{N}[\sigma]^{n-1}\right]}\right). \tag{26}$$

It is known that in the large Hilbert dimension limit, this quantity is almost equal to the original one [24,25]. For a moment, let us focus on the first term of Eq. (26). Using the West-coast notation (15), the trace $\mathrm{tr}\,[\mathcal{N}[\rho]^n]$ can be written in terms of overlaps,

$$\mathrm{tr}\,[\mathcal{N}[\rho]^n] = \frac{1}{(k\,d_C)^n}\sum_{\boldsymbol{i}=1}^{k}\sum_{\boldsymbol{T},\tilde{\boldsymbol{T}}=1}^{d_T}\prod_{m=0}^{n-1}\left(\left\langle\psi_{i_m}^{\tilde{T}_m}|\psi_{i_{m+1}}^{T_m}\right\rangle\,\rho_{T_m\tilde{T}_m}\right), \tag{27}$$

where $i_0 = i_n$, and the bold fonts $\boldsymbol{i}$, $\boldsymbol{T}$ in the summation symbol mean the sum with respect to the set of indices; $\sum_{\boldsymbol{i}=1}^{k} = \sum_{i_0=1}^{k}\cdots\sum_{i_{n-1}=1}^{k}$.

In computing the Rényi entropy (27) we need to evaluate the product of overlaps $\prod_{m=0}^{n-1}\langle\psi_{i_m}^{\tilde{T}_m}|\psi_{i_{m+1}}^{T_m}\rangle$ with $|\psi_{i_n}^{T}\rangle \equiv |\psi_{i_0}^{T}\rangle$ and its Haar random average. We do this using the diagrammatic technique introduced in the previous section.

Among all possible diagrams, we are particularly interested in the ones dominating the sum, both in early times ($d_D \ll d_T$) and in late times ($d_D \gg d_T$). We now argue that the fully disconnected diagram (the left panel of Fig. 3), where, for all EoW branes, the starting point and endpoint are on the same interval, dominates in early times, and the fully connected diagram (the right panel of Fig. 3), where the indices form a single loop, dominates in late times by explicit calculations. The calculation here is very similar to the ones in Refs. [4,25].

First, let us evaluate the contribution of the fully disconnected diagram. Since the contribution of this diagram is evaluated as

$$\left(\overline{\prod_{m=0}^{n-1}\left\langle\psi_{i_m}^{\tilde{T}_m}|\psi_{i_{m+1}}^{T_m}\right\rangle}\right)_{\mathrm{discon}} = d_C^n\prod_{m=0}^{n-1}\left(\delta_{i_m i_{m+1}}\delta_{\tilde{T}_m T_m}\right), \tag{28}$$

the contribution of this diagram to the Rényi entropy is

$$\overline{\mathrm{tr}\,[\mathcal{N}[\rho]^n]}\Big|_{\text{fully discon}} = \frac{1}{(k\,d_C)^n}\cdot k\,(d_C)^n\sum_{\boldsymbol{T}=1}^{d_T}\rho_{T_1T_1}\,\rho_{T_2T_2}\cdots\rho_{T_nT_n} = \frac{1}{(k)^{n-1}}\left(\mathrm{tr}\,[\rho]\right)^n. \tag{29}$$

Similarly, the value of the fully connected diagram is given by

$$\left(\overline{\prod_{m=0}^{n-1}\left\langle \psi_{i_m}^{\tilde{T}_m}|\psi_{i_{m+1}}^{T_m}\right\rangle}\right)_{\text{fully conn}} = d_C\prod_{m=0}^{n-1}\left(\delta_{\tilde{T}_{m+1}T_m}\right) \Rightarrow \left.\overline{\text{tr}\,[\mathcal{N}[\rho]^n]}\right|_{\text{fully conn}} = \frac{1}{(d_C)^{n-1}}\,\text{tr}\,[\rho^n]\,. \tag{30}$$

Combining these two results, $\overline{\text{tr}\,[\mathcal{N}[\rho]^n]}$ is given by

$$\overline{\text{tr}\,[\mathcal{N}[\rho]^n]} = \frac{1}{(k)^{n-1}}\,(\text{tr}\,[\rho])^n + \frac{1}{(d_C)^{n-1}}\,\text{tr}\,[\rho^n] + \cdots\,, \tag{31}$$

where $\cdots$ means contributions coming from partially connected saddles.

Since there are upper and lower bounds on $\text{tr}\,[\rho^n]$, i.e. $1/(d_T)^{n-1} \le \text{tr}\,[\rho^n] \le 1$, we can see that

$$\begin{aligned}\overline{\text{tr}\,[\mathcal{N}[\rho]^n]} &= \frac{1}{(k)^{n-1}}\,(\text{tr}\,[\rho])^n + \frac{1}{(d_C)^{n-1}}\,\text{tr}\,[\rho^n] + \cdots\,,\\ &\approx \begin{cases}\dfrac{1}{(k)^{n-1}} & k \ll d_C \Leftrightarrow d_T \ll \left(\dfrac{d_T}{d_D}\right)^2\\ \dfrac{1}{(d_C)^{n-1}}\,\text{tr}\,[\rho^n] & d_C\,d_T \ll k \Leftrightarrow \left(\dfrac{d_T}{d_D}\right)^2 \ll 1\end{cases}.\end{aligned} \tag{32}$$

Thus, when the necessary condition for the decoupling condition, $d_T/d_D \ll 1$, holds, the dominant contribution is given by the fully connected saddle.

We have to carefully evaluate the precise range of m where the value of the connected saddle gets larger than that of the disconnected saddle. This value of m depends on the density matrix ρ on the code subspace, and gets maximized when it is the maximally mixed state $\rho = I_T/d_T$. Therefore, after $k > d_C d_T$, the connected saddle becomes the dominant one for all density matrices in H_{code}.

Next, let us evaluate the second term of Eq. (26). This computation is completely parallel to the above computation. In terms of the overlaps, it is given by

$$\text{tr}\left[\mathcal{N}[\rho]\mathcal{N}[\sigma]^{n-1}\right] = \frac{1}{(k\,d_C)^n}\sum_{\boldsymbol{i}=1}^{k}\sum_{\boldsymbol{T},\tilde{\boldsymbol{T}}=1}^{d_T}\left(\prod_{m=0}^{n-1}\langle\psi_{i_m}^{\tilde{T}_m}|\psi_{i_{m+1}}^{T_m}\rangle\right)\,\rho_{T_0\,\tilde{T}_0}\left(\prod_{m=1}^{n-1}\sigma_{T_m\,\tilde{T}_m}\right). \tag{33}$$

The contribution of the fully disconnected diagram and the connected diagram to the second term of Eq. (26) can be evaluated, again by substituting the result using Eqs. (28) and (30):

$$\begin{aligned}\text{tr}\left[\mathcal{N}[\rho]\mathcal{N}[\sigma]^{n-1}\right]\big|_{\text{discon}} &= \frac{1}{(k)^{n-1}}\;\text{tr}\,[\rho]\;(\text{tr}\,[\sigma])^{n-1}\,,\\ \overline{\text{tr}\left[\mathcal{N}[\rho]\mathcal{N}[\sigma]^{n-1}\right]}\big|_{\text{conn}} &= \frac{1}{(d_C)^{n-1}}\,\text{tr}\left[\rho\,\sigma^{n-1}\right].\end{aligned} \tag{34}$$

Thus, using these results, we obtain

$$\begin{aligned}\overline{\text{tr}\left[\mathcal{N}[\rho]\mathcal{N}[\sigma]^{n-1}\right]} &= \frac{1}{(k)^{n-1}}\,\text{tr}\,[\rho]\,(\text{tr}\,[\sigma])^{n-1} + \frac{1}{(d_C)^{n-1}}\,\text{tr}\left[\rho\sigma^{n-1}\right] + \cdots\,,\\ &\approx \begin{cases}\dfrac{1}{(k)^{n-1}} & k \ll d_C \Leftrightarrow d_T \ll \left(\dfrac{d_T}{d_D}\right)^2\\ \dfrac{1}{(d_C)^{n-1}}\,\text{tr}\left[\rho\sigma^{n-1}\right] & k \gg d_C d_T \Leftrightarrow \left(\dfrac{d_T}{d_D}\right)^2 \ll 1\end{cases},\end{aligned} \tag{35}$$

where $\cdots$ again means contributions coming from partially connected saddles, and also in the second approximate equality, we assumed that $1/(d_T)^{n-1} \lesssim \mathrm{tr}\left[\rho\sigma^{n-1}\right] \leq 1$ in order to obtain the conditions.[11]

Now that we have evaluated the two terms that appeared in the relative entropy, we can obtain the resulting relative entropy:

$$\begin{aligned}\overline{S(\mathcal{N}[\rho]||\mathcal{N}[\sigma])} &\approx \lim_{n\to 1}\frac{1}{n-1}\left(\log\overline{\mathrm{tr}\,[\mathcal{N}[\rho]^n]} - \log\overline{\mathrm{tr}\left[\mathcal{N}[\rho]\mathcal{N}[\sigma]^{n-1}\right]}\right),\\ &\approx \begin{cases} 0 & k \ll d_C \Leftrightarrow d_T \ll \left(\frac{d_T}{d_D}\right)^2 \\ \lim_{n\to 1}\frac{1}{n-1}\left(\log\mathrm{tr}\,[\rho^n] - \log\mathrm{tr}\left[\rho\sigma^{n-1}\right]\right) & k \gg d_C d_T \Leftrightarrow \left(\frac{d_T}{d_D}\right)^2 \ll 1 \end{cases}\\ &= \begin{cases} 0 & k \ll d_C \Leftrightarrow d_T \ll \left(\frac{d_T}{d_D}\right)^2 \\ S(\rho||\sigma) & k \gg d_C d_T \Leftrightarrow \left(\frac{d_T}{d_D}\right)^2 \ll 1. \end{cases}\end{aligned} \tag{36}$$

Thus we can conclude that, when the condition $d_T/d_D \ll 1$ is satisfied, the relative entropies obey the relation

$$\overline{S(\mathcal{N}[\rho]||\mathcal{N}[\sigma])} \approx S(\rho||\sigma). \tag{37}$$

This result implies that the condition of sufficiency holds for the HP channel when $\left(\frac{d_T}{d_D}\right)^2 \ll 1$.

3.1. *Check the recovery map*

We argued that in chaotic systems, the Petz recovery map (6) gets simplified and is reduced to the so-called Petz-lite map $\mathcal{R}^{\mathrm{Lite}}$ defined in Eq. (12). In this section, we show this by checking

$$\overline{S(\mathcal{R}^{\mathrm{Lite}}[\mathcal{N}[\rho_T]]\,||\rho_T)} = 0, \quad \text{when } \left(\frac{d_T}{d_D}\right)^2 \ll 1 \tag{38}$$

for any density matrix ρ_T on the code subspace. This means that at sufficiently late times, one can recover ρ_T from the state of the Hawking radiation $\mathcal{N}[\rho_T]$ by applying the recovery map $\mathcal{R}^{\mathrm{Lite}}$.

One can show this by computing the relative entropy by the replica trick similar to Eq. (25),

$$\overline{S(\mathcal{R}^{\mathrm{Lite}}[\mathcal{N}[\rho_T]]\,||\rho_T)} = \lim_{n\to 1}\frac{1}{n-1}\left(\log\overline{\mathrm{tr}(\mathcal{R}^{\mathrm{Lite}}[\mathcal{N}[\rho]])^n} - \log\overline{\mathrm{tr}(\mathcal{R}^{\mathrm{Lite}}[\mathcal{N}[\rho]]\,\rho^{n-1})}\right). \tag{39}$$

In terms of Haar random unitaries, $\mathcal{R}^{\mathrm{Lite}}[\mathcal{N}[\rho_T]]$ is given by

$$\begin{aligned}\mathcal{R}^{\mathrm{Lite}}[\mathcal{N}[\rho_T]] &= \frac{1}{N}\cdot\frac{d_B d_D}{d_T}\cdot\mathcal{N}^{\dagger}_{D,B\to T}[\mathcal{N}_{T\to D,B}[\rho]]\\ &= \frac{1}{N}\sum_{\tilde{T},\tilde{T}'=1}^{d_T}|\tilde{T}\rangle_T\langle\tilde{T}'|\cdot\frac{1}{k(d_C)^2 d_T}\sum_{T,T'=1}^{d_T}\sum_{i,j=1}^{k}\left\langle\psi_i^{\tilde{T}}\middle|\psi_j^{\tilde{T}'}\right\rangle\left\langle\psi_j^{T'}\middle|\psi_i^{T}\right\rangle(\rho)_{TT'}.\end{aligned} \tag{40}$$

Therefore, the first term in Eq. (39) is given by

$$\mathrm{tr}(\mathcal{R}^{\mathrm{Lite}}[\mathcal{N}[\rho]])^n = \frac{1}{(Nkd_C^2 d_T)^n}\sum_{\boldsymbol{T},\boldsymbol{T}'=1}^{d_T}\sum_{\tilde{\boldsymbol{T}},\tilde{\boldsymbol{T}}'=1}^{d_T}\sum_{\boldsymbol{i},\boldsymbol{j}=1}^{k}\prod_{m=1}^{n}\left(\left\langle\psi_{i_m}^{T_m}\middle|\psi_{j_m}^{T_{m+1}}\right\rangle\left\langle\psi_{j_m}^{\tilde{T}_m}\middle|\psi_{i_m}^{\tilde{T}'_m}\right\rangle\rho_{\tilde{T}_m\tilde{T}'_m}\right). \tag{41}$$

[11] If the support of the density matrix ρ is not contained in that of σ, then $\mathrm{tr}\left[\rho\sigma^{n-1}\right] = 0$, implying the divergent relative entropy $S(\rho||\sigma) = \infty$. In that case, we would need another treatment, thus we do not consider such a case in this paper.

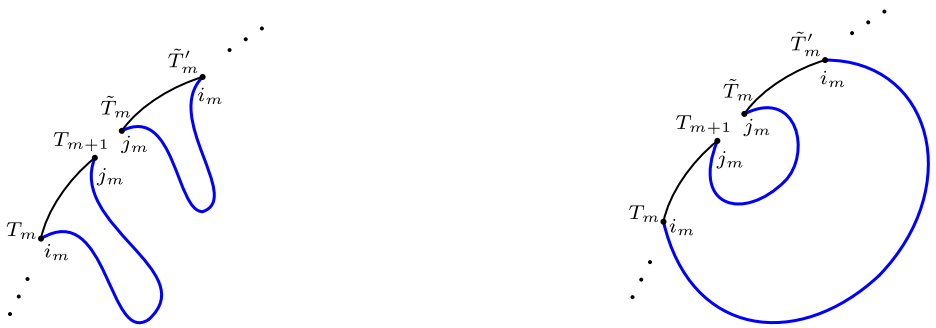

Fig. 4. Diagrams for the product of overlaps appearing in the calculation of Eq. (41). Left: Disconnected diagram. Right: The connected diagram.

We compute this by following the procedure explained in Sect. 2.1, namely by preparing an interval for each overlap, and connecting the endpoints of the intervals by EoW branes, then evaluating each diagram generated in this way. As shown in Fig. 4, the m-th replica consists of two intervals with indices for Hawking radiation i_m, j_m. Therefore, it is clear that when $k = d_D d_B$ is sufficiently large, the dominant diagram is the one connecting the endpoint with the index i_m in the first interval to the endpoint of the second replica with the same index in the same replica (the right panel of Fig. 4). Similarly, we connect the endpoints with j_m in this replica. This is because, if there is an EoW brane connecting endpoints with distinct Hawking indices (say i, j), then the value of the diagram is significantly reduced in the large-k limit because of the Kronecker delta factor δ_{ij} coming from the EoW brane.

This means that in the dominant saddle, two different replicas are not connected by any EoW brane, because they start and end at the same replica. This means that the Rényi entropy is a self-averaging quantity:

$$\overline{\mathrm{tr}(\mathcal{R}^{\mathrm{Lite}}[\mathcal{N}[\rho]])^n} = \mathrm{tr}\left(\overline{\mathcal{R}^{\mathrm{Lite}}[\mathcal{N}[\rho]]}\right)^n . \tag{42}$$

A similar statement holds for the second term of Eq. (39); therefore, we conclude that the relative entropy of our interest is also self-averaging,

$$\overline{S(\mathcal{R}^{\mathrm{Lite}}[\mathcal{N}[\rho_T]] \,||\rho_T)} = S(\overline{\mathcal{R}^{\mathrm{Lite}}[\mathcal{N}[\rho_T]]}\,||\rho_T), \tag{43}$$

when k is sufficiently large. This implies that in the relative entropy, one can replace $\mathcal{R}^{\mathrm{Lite}}[\mathcal{N}[\rho_T]]$ with its average $\overline{\mathcal{R}^{\mathrm{Lite}}[\mathcal{N}[\rho_T]]}$. The average of the density matrix is given by

$$\overline{\mathcal{R}^{\mathrm{Lite}}[\mathcal{N}[\rho_T]]} = \frac{1}{1+\left(\frac{d_T}{d_D}\right)^2}\left(\rho + \left(\frac{d_T}{d_D}\right)^2 \cdot \frac{I_T}{d_T}\right). \tag{44}$$

A more precise way to argue this is the following: Let us compute

$$\overline{\mathrm{tr}\left[\left(\mathcal{R}^{\mathrm{Lite}}[\mathcal{N}[\rho_T]] - \overline{\mathcal{R}^{\mathrm{Lite}}[\mathcal{N}[\rho_T]]}\right)^2\right]} = \overline{\mathrm{tr}\left[\left(\mathcal{R}^{\mathrm{Lite}}[\mathcal{N}[\rho_T]]\right)^2\right]} - \mathrm{tr}\left[\left(\overline{\mathcal{R}^{\mathrm{Lite}}[\mathcal{N}[\rho_T]]}\right)^2\right]. \tag{45}$$

Then, the right-hand side of the above equation is given by

$$\frac{(k\,d_C)^4}{\left(Nk(d_C)^2 d_T\right)^2}\left\{\frac{1}{k\,d_C}\left[\frac{1}{k^2}\left(2+d_T\,\mathrm{tr}\left[\rho^2\right]+(d_T)^2\right)\right.\right.$$
$$\left.\left.+\frac{1}{k\,d_C}\left((d_T)^2\,\mathrm{tr}\left[\rho^2\right]+2d_T+2\,\mathrm{tr}\left[\rho^2\right]\right)+\frac{1}{(d_C)^2}d_T\,\mathrm{tr}\left[\rho^2\right]\right]\right\}, \tag{46}$$

which becomes small when $k \gg d_C d_T$. By plugging this expression, we have

$$\overline{S(\mathcal{R}^{\mathrm{Lite}}[\mathcal{N}[\rho_T]]\,||\rho_T)} \approx S(\overline{\mathcal{R}^{\mathrm{Lite}}[\mathcal{N}[\rho_T]]}\,||\rho_T)$$
$$= \begin{cases} S\left(\rho\left\|\frac{I_T}{d_T}\right.\right) & k \ll d_C \Leftrightarrow d_T \ll \left(\frac{d_T}{d_D}\right)^2 \\ 0 & k \gg d_C d_T \Leftrightarrow \left(\frac{d_T}{d_D}\right)^2 \ll 1. \end{cases} \tag{47}$$

Thus, for early times $k \ll d_C$, the relative entropy is nonvanishing unless $\rho = I_T/d_T$, but for late times $d_C\,d_T \ll k$, the relative entropy is vanishing. This result implies that when $k \gg d_C d_T$, $\mathcal{R}^{\mathrm{Lite}}$ indeed works as a recovery map.

3.2. *Relation to the YK protocol*

So far, we have shown that when $k \gg d_C d_T$, the Petz-lite $\mathcal{R}^{\mathrm{Lite}} \sim \mathcal{N}^\dagger$ indeed works as a recovery map. However, we have not discussed the physical interpretation of the Petz-lite. Thus, in this subsection, we explain the interpretation by showing the equivalence between the Petz-lite and the well-known YK protocol. The relation between the YK protocol and the Petz map has been suggested by Yoshida [12,13].

In Ref. [17], Yoshida and Kitaev proposed an interesting recovery protocol for the object thrown into the black hole T from late and early radiation DB. A brief summary of their protocol is as follows:

(1) In addition to the original HP setup, introduce a copy of the diary and the reference, denoted by $R'T'$. We choose the state on $R'T'$ to be an EPR state. Bob can manipulate Hawking radiation DB and $R'T'$. Before applying the decoding protocol, the state of the total system is

$$|\Psi_{\mathrm{HP}}\rangle \otimes |\mathrm{EPR}\rangle_{R'T'}, \tag{48}$$

where $|\Psi_{\mathrm{HP}}\rangle$ is the state on $RCDB$ given by Eq. (2).

(2) We then use the early Hawking radiation B and the copy of the diary T' to simulate the black hole dynamics by applying U^*, which is the complex conjugate of U for the time evolution of the original system. After the simulation, the total system consists of $RCDR'C'D'$, and the state is

$$|\Psi_{\mathrm{YK}}\rangle_{RCDD'C'R'} = \left(I_{RC}\otimes I_D \otimes U^*_{D'C'\to BT'}\otimes I_R\right)|\Psi_{HP}\rangle \otimes |\mathrm{EPR}\rangle_{R'T'}. \tag{49}$$

(3) Postselect to the EPR pair on DD'. If it succeeds, the state on RR' is the EPR state with high fidelity, meaning information recovery has been successful.

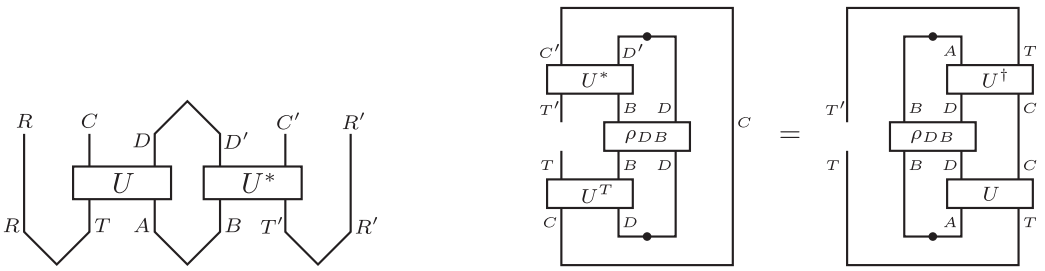

Fig. 5. Left: YK decoding protocol. Right: Operator transpose that provides the key equivalence (55).

The quantum circuit for the protocol is shown in the left panel of Fig. 5. Combining these steps, the quantum channel $\mathcal{R}^{YK}_{D,B\to R'}$ for the YK recovery map is given by

$$\begin{aligned}&\mathcal{R}^{\mathrm{YK}}_{D,B\to R'}\left[\mathcal{O}_{DB}\right]\\&=\frac{1}{N_{\mathrm{YK}}}\,\mathrm{tr}_{C'}\left[{}_{D,D'}\langle \mathrm{EPR}|\, U^{*}_{B,T'\to C',D'}\left(\mathcal{O}_{DB}\otimes|\mathrm{EPR}\rangle_{T',R'}\langle\mathrm{EPR}|\right)U^{T}_{B,T'\to C',D'}\,|\mathrm{EPR}\rangle_{D,D'}\right],\end{aligned}\tag{50}$$

where N_{YK} is a normalization factor given by

$$N_{\mathrm{YK}}=\overline{\left|{}_{D,D'}\langle\mathrm{EPR}|\Psi_{YK}\rangle\right|^2}\approx\frac{1}{(d_T)^2}+\frac{1}{(d_D)^2}.\tag{51}$$

For the above YK recovery map, we show the equivalence between the YK recovery map $\mathcal{R}^{\mathrm{YK}}_{D,B\to R'}$ and the Petz-lite (10), $\mathcal{R}^{\mathrm{Lite}}_{D,B\to T}$, up to the isomorphism $V_{T\to R'}$ between systems T and R',

$$\mathcal{R}^{YK}_{D,B\to R'}\left[\mathcal{O}_{DB}\right]=V_{T\to R'}\,\mathcal{R}^{\mathrm{Lite}}_{D,B\to T}\left[\mathcal{O}_{DB}\right]\,V^{\dagger}_{T\to R'},\tag{52}$$

where $V_{T\to R'}$ is explicitly given by

$$V_{T\to R'}\coloneqq d_T\;{}_{T,T'}\langle\mathrm{EPR}|\mathrm{EPR}\rangle_{T',R'}=\sum_{\tilde{T}=1}^{d_T}\left|\tilde{T}\right\rangle_{R'}{}_{T}\!\left\langle\tilde{T}\right|.\tag{53}$$

The argument for the equivalence is summarized in the right panel of Fig. 5. We start with the YK recovery map (50). First, we rewrite the trace of subsystem C' in the YK recovery map as

$$\mathrm{tr}_{C'}\left[\mathcal{O}\right]=d_C\;{}_{C,C'}\langle\mathrm{EPR}|\left(I_C\otimes\mathcal{O}\right)|\mathrm{EPR}\rangle_{C,C'},\tag{54}$$

and introduce two EPR states $|\mathrm{EPR}\rangle_{D,D'}$ and $|\mathrm{EPR}\rangle_{C,C'}$.

Next, by using Eq. (54) and the relation (see Appendix B for the derivation):

$$U^{T}_{C',D'\to B,T'}\,|\mathrm{EPR}\rangle_{C,C'}\otimes|\mathrm{EPR}\rangle_{D,D'}=U_{A,T\to C,D}\,|\mathrm{EPR}\rangle_{A,B}\otimes|\mathrm{EPR}\rangle_{T,T'},\tag{55}$$

the YK recovery map (52) can be rewritten as

$$\begin{aligned}
&\mathcal{R}^{YK}_{D,B\to R'}[\mathcal{O}_{DB}] \\
&= \frac{d_C}{N_{\rm YK}} \left({}_{A,B}\langle \mathrm{EPR}| \otimes {}_{T,T'}\langle \mathrm{EPR}| \right) \left[U^\dagger_{A,T\to C,D} \left(\mathcal{O}_{DB} \otimes |\mathrm{EPR}\rangle_{T',R'} \langle \mathrm{EPR}| \right) U_{A,T\to C,D} \right] \\
&\quad \times \left(|\mathrm{EPR}\rangle_{A,B} \otimes |\mathrm{EPR}\rangle_{T,T'} \right) \\
&= \frac{d_C}{N_{\rm YK}} \left({}_{T,T'}\langle \mathrm{EPR}|\mathrm{EPR}\rangle_{T',R'} \right) \\
&\quad \times {}_{A,B}\langle \mathrm{EPR}| \left[U^\dagger_{T,A\to C,D}\, \mathcal{O}_{DB}\, U_{T,A\to C,D} \right] |\mathrm{EPR}\rangle_{A,B} \\
&\quad \times \left({}_{T',R'}\langle \mathrm{EPR}|\mathrm{EPR}\rangle_{T,T'} \right) \\
&= \frac{d_C}{(d_T)^2 N_{\rm YK}} V_{T\to R'} \mathcal{N}^\dagger_{D,B\to T,A}[\mathcal{O}_{D,B}]\, V^\dagger_{T\to R'},
\end{aligned} \tag{56}$$

where in the final line, we used the definition of the isomorphism (53) and the adjoint HP channel (7). Additionally, the above overall constant $\frac{d_C}{(d_T)^2 N_{\rm YK}}$ coincides with that of the Petz-lite (12), since

$$\frac{d_C}{(d_T)^2 N_{\rm YK}} = \frac{d_C}{1 + \left(\frac{d_T}{d_D} \right)^2}, \tag{57}$$

where we used the definition of $N_{\rm YK}$, Eq. (51). Therefore, the above expression implies the desired relation (52).

4. Recovery map for the HP channel in SYK

So far, we have given the evidence that the Petz-lite works as a recovery map under the Haar random unitary, which is highly chaotic. In this section, we argue that this continues to hold for a more realistic but tractable model of chaotic dynamics: the SYK model [26–28]. In this paper, we briefly explain the relevant calculations, leaving details for an upcoming paper [16].

4.1. *Setup of the SYK HP protocol*

In this section, we explain the setup to study the HP-like protocol (what we call the SYK HP channel) in the SYK model. This was first introduced in Refs. [14,29].

The SYK model is a theory of N Majorana fermions ψ_i, and its Hamiltonian is given by

$$H = (i)^{q/2} \sum_{1\le i_1<i_2<\cdots<i_q\le N} j_{i_1 i_2\cdots i_q} \psi_{i_1} \psi_{i_2} \cdots \psi_{i_q}, \tag{58}$$

where $q \in 2\mathbb{N}\,(q > 2)$, $j_{i_1 i_2\cdots i_q}$ is a random coefficient drawn from a Gaussian random distribution with zero mean and the variance $\left\langle j^2_{i_1 i_2\cdots i_q} \right\rangle = J^2 (q-1)!/N^{q-1}$.

Following Ref. [14], we consider two copies of the Hilbert space of the SYK model, say, a left SYK system L and a right one R. Hereafter, we denote the Majorana fermions on the left system by $\psi_{i,L}$ and $\psi_{i,R}$ for the right. For notational simplicity, we use the convention

$$\left\{ \psi_i, \psi_j \right\} = 2\delta_{i,j}, \tag{59}$$

for the anticommutation relation for the fermions on the same side. In this setup, the right SYK system corresponds to early radiation degrees of freedom of the original HP setup, and the left SYK system corresponds to the rest: the union of the diary system and the initial black hole before the action of the random unitary, or equivalently the remaining black hole plus late radiation degrees of freedom after the unitary evolution. In particular, the left system L is divided into two subsystems, say, $\tilde{L}$ and K; the former corresponds to the remaining black hole, and the latter to the late radiation part of the original HP setup.

On the union of the above SYK systems L and R, we consider the following thermo-field double (TFD) state:

$$|\mathrm{TFD}\rangle_{L,R} = Z^{-1/2}(\beta)\, e^{-\beta(H_L+H_R)/4}\, |0\rangle_{L,R}\,, \tag{60}$$

where $Z(\beta)$ is a normalization factor of the state, and $|0\rangle_{L,R}$ is given by [30]:

$$\left[\, \psi_{j,L}(0) + i\psi_{j,R}(0)\,\right] |0\rangle_{L,R} = 0 \quad \text{for } \forall j. \tag{61}$$

Note that the TFD state (60) satisfies the relation $(H_L - H_R)\,|\mathrm{TFD}\rangle = 0$. This TFD state corresponds to an entangled state between the initial black hole and the early radiation.

The code subspace (a diary system) of our interest is 2D, and let us denote two basis vectors by $|0\rangle$ and $|1\rangle$. This code subspace is embedded into the physical Hilbert space LR by an isometry. The image of the code subspace is spanned by the TFD state $|\mathrm{TFD}\rangle_{L,R}$ and the excited state $\psi_{i,L}(0)\,|\mathrm{TFD}\rangle_{L,R}$. Here, we assume that the Majorana fermion $\psi_{i,L}(0)$ acting on the TFD state lives in the subsystem $\tilde{L}$, $i \in \tilde{L}$. More explicitly, by the isometry, the states in the code subspace $|T\rangle$ $(T = 0, 1)$ are mapped to

$$(V_{T,L\to L} \otimes I_R)\left(|T\rangle_T \otimes |\mathrm{TFD}\rangle_{L,R}\right) \coloneqq \begin{cases} |\mathrm{TFD}\rangle_{L,R} & \text{for } T = 0 \\ \dfrac{1}{(Z_\delta)^{\frac{1}{2}}}\psi_{i,L}(i\delta)\,|\mathrm{TFD}\rangle_{L,R} & \text{for } T = 1, \end{cases} \tag{62}$$

where $\psi_{i,L}(i\delta)$ is the regulated Majorana fermion operator

$$\psi_{i,L}(i\delta) = e^{-\delta H_L}\psi_{i,L}(0)e^{\delta H_L}, \tag{63}$$

and δ is an infinitesimal cutoff parameter to normalize the state with the operator insertion even in the conformal limit, where the SYK model has an effective description in terms of the reparametrization modes [31]. Z_δ is its normalization factor given by the two-point function

$$\begin{aligned} Z_\delta &= \frac{1}{N-K}\sum_{i=1}^{N-K}\frac{1}{Z(\beta)}\,\mathrm{tr}\left[e^{-\beta H_L}\psi_{i,L}(-i\delta)\psi_{i,L}(i\delta)\right] \\ &= \frac{1}{N-K}\sum_{i=1}^{N-K}\frac{1}{Z(\beta)}\,\mathrm{tr}\left[e^{-\beta H_L}e^{2\delta H_L}\psi_{i,L}(0)e^{-2\delta H_L}\psi_{i,L}(0)\right] = G_\beta(2\delta). \end{aligned} \tag{64}$$

This normalization factor is not for the specific Majorana fermion "i" but averaged over the region $\tilde{L}$ with $N - K$ sites. We expect that the difference between the two only appears in subleading terms with respect to K/N because of typicality. Therefore, we use this normalization factor (64) for later convenience.

Using the above embedding, we can holographically prepare an initial entangled state between the early radiation and an initial black hole containing a diary in the SYK model. For this system, we consider a unitary time evolution on the left system L by the SYK Hamiltonian H_L,

$$U_L(t) = \exp\left(itH_L\right). \tag{65}$$

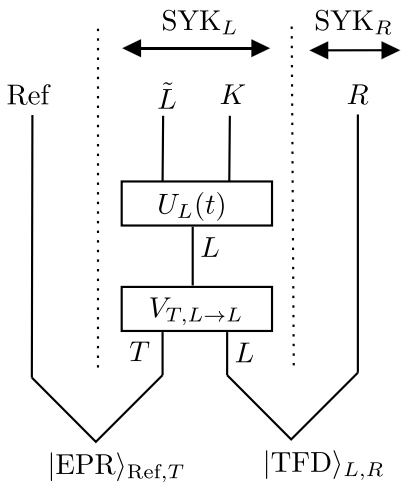

Fig. 6. Circuit diagram corresponding to the state in Eq. (66).

By this time evolution, information in the diary gets scrambled and uniformly distributed over the left SYK system after the scrambling time. The resulting state is

$$|\Psi_{\text{SYK HP}}\rangle = (I_{\text{Ref}} \otimes U_L(t) \otimes I_R)\,(I_{\text{Ref}} \otimes V_{T,L\to L} \otimes I_R)\left(|\text{EPR}\rangle_{\text{Ref},T} \otimes |\text{TFD}\rangle_{L,R}\right), \tag{66}$$

which corresponds to the state in Eq. (2). In Fig. 6, we give the circuit diagram corresponding to the state in Eq. (66).

We are interested in recovering the diary information from the early and late radiations R and K by using the Petz-lite for the SYK HP protocol. As in Eq. (4), the SYK HP channel $\mathcal{N}^{\text{SYK}}_{T\to K,R}$ representing error is obtained by tracing out the remaining black hole part $\tilde{L}$ in the final state (66),

$$\mathcal{N}^{\text{SYK}}_{T\to K,R}[\rho_T] \coloneqq \text{tr}_{\tilde{L}}\left[U_L V_{T,L\to L}\left(\rho_T \otimes |\text{TFD}\rangle_{L,R}\langle\text{TFD}|\right) V^\dagger_{T,L\to L} U^\dagger_L\right]. \tag{67}$$

This channel maps a density matrix on the diary T to the one on the late and early radiation system K, R. Also, the adjoint $\mathcal{N}^{\text{SYK}\dagger}_{K,R\to T}$ of the SYK HP channel is given by

$$\begin{aligned}\mathcal{N}^{\text{SYK}\dagger}_{K,R\to T}[\mathcal{O}_{KR}] &\coloneqq \text{tr}_{L,R}\left[|\text{TFD}\rangle_{L,R}\langle\text{TFD}|\left(V^\dagger_{L\to T,L} U^\dagger_L\,\mathcal{O}_{KR}\,U_L V_{L\to T,L}\right)\right]\\ &= {}_{L,R}\langle\text{TFD}|\left(V^\dagger_{L\to T,L} U^\dagger_L\,\mathcal{O}_{KR}\,U_L V_{L\to T,L}\right)|\text{TFD}\rangle_{L,R}\,.\end{aligned} \tag{68}$$

The above quantum channels are analogous to the original HP channel and its adjoint for the Haar random unitary. However, we note that there is a difference between them in the sense that the SYK HP channel and its adjoint include the embedding map V, which induces (fermionic) excitations.

4.2. *Some matrix elements of the Petz-lite and Rényi-two correlators*

Now that we have prepared the SYK HP channel and its adjoint, we can construct the Petz-lite map for this channel. As in the Petz-lite for the Haar random case (10), we consider the Petz-lite for the SYK case,

$$\mathcal{R}^{\text{Lite,SYK}}_{K,R\to T}[\mathcal{O}_{KR}] = \frac{1}{N_{\text{SYK}}}\mathcal{N}^{\text{SYK}\dagger}_{K,R\to T}[\mathcal{O}_{KR}], \tag{69}$$

where N_{SYK} is the normalization factor, which is determined by the condition

$$\text{tr}_T\left[\mathcal{R}^{\text{Lite,SYK}}_{K,R\to T}\left[\mathcal{N}^{\text{SYK}}_{T\to K,R}[\sigma_T]\right]\right] = 1. \tag{70}$$

Here, σ_T is some reference state in T for the normalization. We take it to be $\sigma_T = |0\rangle_T\langle 0|$. For this choice, the normalization factor is given by

$$N_{\rm SYK} = \sum_{T=0,1} \langle T|\mathcal{N}^{\rm SYK\dagger}_{K,R\to T}\left[\mathcal{N}^{\rm SYK}_{T\to K,R}[|0\rangle_T\langle 0|]\right]|T\rangle\,. \tag{71}$$

We note that due to this normalization, we can see that the Petz-lite (69) for the SYK HP protocol has a similar overall constant to the Petz-lite for the original HP protocol (12). To see the similarity, we first rewrite the Petz-lite (69) with the normalization factor (71) as follows,

$$\mathcal{R}^{\rm Lite,SYK}_{K,R\to T}[\mathcal{O}_{KR}] = \frac{\left\langle \hat{d}_{\tilde{L}}\right\rangle_\beta}{1+\left\langle \hat{d}_{\tilde{L}}\right\rangle_\beta \langle 1|\mathcal{N}^{\rm SYK\dagger}_{K,R\to T}\left[\mathcal{N}^{\rm SYK}_{T\to K,R}[|0\rangle_T\langle 0|]\right]|1\rangle}\mathcal{N}^{\rm SYK\dagger}_{K,R\to T}[\mathcal{O}_{KR}], \tag{72}$$

where $\left\langle \hat{d}_{\tilde{L}}\right\rangle_\beta$ is an effective dimension of subsystem $\tilde{L}$ defined by the purity $\mathrm{tr}_{\tilde{L}}\left[\left(\rho_{\tilde{L}}\right)^2\right]$ of the TFD state with respect to the subsystem,[12]

$$\langle 0|\mathcal{N}^{\rm SYK\dagger}_{K,R\to T}\left[\mathcal{N}^{\rm SYK}_{T\to K,R}[|0\rangle_T\langle 0|]\right]|0\rangle = \mathrm{tr}_{KR}\left[(\rho_{KR})^2\right] = \mathrm{tr}_{\tilde{L}}\left[\left(\rho_{\tilde{L}}\right)^2\right] =: \frac{1}{\left\langle \hat{d}_{\tilde{L}}\right\rangle_\beta}. \tag{73}$$

The effective dimension is analogous to the dimension of the remaining black hole in the original HP setup. Indeed, in the infinite temperature limit $\beta\to 0$, the effective dimension is almost reduced to the actual dimension of subsystem $\tilde{L}$, $d_{\tilde{L}} = 2^{\frac{N-K}{2}}$.[13] However, in general, the effective dimension is smaller than the actual dimension due to the property of the purity and thermal effects;

$$1 \le \left\langle \hat{d}_{\tilde{L}}\right\rangle_\beta \le d_{\tilde{L}}, \tag{74}$$

where this effective dimension becomes closed to 1 in $\beta\to\infty$ and $d_{\tilde{L}}$ in $\beta\to 0$. With this effective dimension, we can compare the Petz-lite (72) for the SYK model to that for the original one (12) in the HP setup

$$\mathcal{R}^{\rm Lite,HP}_{D,B\to T}[\mathcal{O}_{DB}] = \frac{d_C}{1+\left(\frac{d_T}{d_D}\right)^2}\mathcal{N}^\dagger_{D,B\to T}[\mathcal{O}_{DB}]\,.$$

The similarities between the quantities in the HP and the SYK are summarized in the following identifications:

$$\begin{aligned} d_C \quad &\longleftrightarrow \quad \left\langle \hat{d}_{\tilde{L}}\right\rangle_\beta, \\ \left(\frac{d_T}{d_D}\right)^2 \quad &\longleftrightarrow \quad \left\langle \hat{d}_{\tilde{L}}\right\rangle_\beta \cdot \langle 1|\mathcal{N}^{\rm SYK\dagger}_{K,R\to T}\left[\mathcal{N}^{\rm SYK}_{T\to K,R}[|0\rangle_T\langle 0|]\right]|1\rangle\,. \end{aligned} \tag{75}$$

Also, we have the unitarity constraint on the dimensions of the Hilbert spaces, $d_T\,d_B = d_C\,d_D$. By using the relation, we can rewrite the dimension as

$$\left(\frac{d_T}{d_D}\right)^2 = \frac{d_C\,d_T}{d_B\,d_D}, \tag{76}$$

[12] We note that in our setting, subsystem $\tilde{L}$ is smaller than the complement system KR.

[13] For Majorana fermions, an annihilation operator is constructed from two Majorana fermions, and the corresponding creation operator is given by the Hermitian conjugation. In other words, two Majorana fermions form a single qubit. Thus, a Hilbert space constructed from m Majorana fermions becomes a $2^{m/2}$-dimensional Hilbert space. See, e.g. Ref. [32] for the review.

from which we have the following identification:

$$\langle 1|\mathcal{N}^{\mathrm{SYK}\dagger}_{K,R\to T}\left[\mathcal{N}^{\mathrm{SYK}}_{T\to K,R}[|0\rangle_T\langle 0|]\right]|1\rangle \quad \longleftrightarrow \quad \frac{1}{d_C}\cdot\left(\frac{d_T}{d_D}\right)^2=\frac{d_T}{d_B\,d_D}=\frac{d_T}{k}. \tag{77}$$

This might be a good ratio to understand current physics; if we have a sufficiently large amount of Hawking radiation compared with the diary, $d_T \ll d_B\,d_D = k$, the ratio becomes almost 0. As we will soon see, the left quantity also becomes almost 0 around and after a critical time.

With this discussion of the normalization factor in mind, we consider a matrix element of $\mathcal{R}^{\mathrm{Lite,SYK}}_{K,R\to T}\left[\mathcal{N}^{\mathrm{SYK}}_{T\to K,R}[\rho_T]\right]$ for a general density matrix ρ_T in the Hilbert space of the diary,

$$\left\langle T\middle|\mathcal{R}^{\mathrm{Lite,SYK}}_{K,R\to T}\left[\mathcal{N}^{\mathrm{SYK}}_{T\to K,R}[\rho_T]\right]\middle|T'\right\rangle. \tag{78}$$

To check whether the Petz-lite works as the recovery map, it is sufficient to see whether the following relation holds (approximately) or not:

$$\left\langle T\middle|\mathcal{R}^{\mathrm{Lite,SYK}}_{K,R\to T}\left[\mathcal{N}^{\mathrm{SYK}}_{T\to K,R}[\rho_T]\right]\middle|T'\right\rangle \overset{?}{\approx} \left\langle T\middle|\rho_T\middle|T'\right\rangle \quad \text{for } \forall\rho_T. \tag{79}$$

Checking the above relation is equivalent to focusing on the matrix elements

$$\left\langle T\middle|\mathcal{R}^{\mathrm{Lite,SYK}}_{K,R\to T}\left[\mathcal{N}^{\mathrm{SYK}}_{T\to K,R}\left[\middle|\tilde{T}\right\rangle_T\left\langle\tilde{T}'\middle|\right]\right]\middle|T'\right\rangle \overset{?}{\approx} \left\langle T\middle|\tilde{T}\right\rangle\left\langle\tilde{T}'\middle|T'\right\rangle, \qquad \forall T, T', \tilde{T}, \tilde{T}'. \tag{80}$$

Generally, we have 16 components of the above matrix, but half of them, including odd Majorana fermions, are trivially vanishing due to the fermionic parity of the SYK model. In other words, matrix elements which satisfy $(T + T' + \tilde{T} + \tilde{T}') \equiv 1 \mod 2$ are vanishing.

Now, we focus on three nonzero matrix elements, and briefly explain how we can evaluate them.[14] First, we consider the $T, T', \tilde{T}, \tilde{T}' = 0$ case. If Eq. (80) holds then since its right-hand side is 1, therefore the following identity holds:

$$1 \overset{?}{\approx} \langle 0|\mathcal{R}^{\mathrm{Lite,SYK}}_{K,R\to T}\left[\mathcal{N}^{\mathrm{SYK}}_{T\to K,R}[|0\rangle_T\langle 0|]\right]|0\rangle = \left(1+\left\langle\hat{d}_{\tilde{L}}\right\rangle_\beta\cdot\langle 1|\mathcal{N}^{\mathrm{SYK}\dagger}_{K,R\to T}\left[\mathcal{N}^{\mathrm{SYK}}_{T\to K,R}[|0\rangle_T\langle 0|]\right]|1\rangle\right)^{-1}. \tag{81}$$

The second one is for the $T, T' = 1, \tilde{T}, \tilde{T}' = 0$ case, where the matrix element is expected to become 0. In this case, we can see that this matrix element has the same ratio as above,

$$0 \overset{?}{\approx} \langle 1|\mathcal{R}^{\mathrm{Lite,SYK}}_{K,R\to T}\left[\mathcal{N}^{\mathrm{SYK}}_{T\to K,R}[|0\rangle_T\langle 0|]\right]|1\rangle = \frac{\left\langle\hat{d}_{\tilde{L}}\right\rangle_\beta\cdot\langle 1|\mathcal{N}^{\mathrm{SYK}\dagger}_{K,R\to T}\left[\mathcal{N}^{\mathrm{SYK}}_{T\to K,R}[|0\rangle_T\langle 0|]\right]|1\rangle}{1+\left\langle\hat{d}_{\tilde{L}}\right\rangle_\beta\cdot\langle 1|\mathcal{N}^{\mathrm{SYK}\dagger}_{K,R\to T}\left[\mathcal{N}^{\mathrm{SYK}}_{T\to K,R}[|0\rangle_T\langle 0|]\right]|1\rangle}. \tag{82}$$

The final one is for $T, \tilde{T} = 0, T', \tilde{T}' = 1$, where the matrix element (80), which is expected to be 1, becomes

$$1 \overset{?}{\approx} \langle 0|\mathcal{R}^{\mathrm{Lite,SYK}}_{K,R\to T}\left[\mathcal{N}^{\mathrm{SYK}}_{T\to K,R}[|0\rangle_T\langle 1|]\right]|1\rangle = \frac{\left\langle\hat{d}_{\tilde{L}}\right\rangle_\beta\cdot\langle 0|\mathcal{N}^{\mathrm{SYK}\dagger}_{K,R\to T}\left[\mathcal{N}^{\mathrm{SYK}}_{T\to K,R}[|0\rangle_T\langle 1|]\right]|1\rangle}{1+\left\langle\hat{d}_{\tilde{L}}\right\rangle_\beta\cdot\langle 1|\mathcal{N}^{\mathrm{SYK}\dagger}_{K,R\to T}\left[\mathcal{N}^{\mathrm{SYK}}_{T\to K,R}[|0\rangle_T\langle 0|]\right]|1\rangle}. \tag{83}$$

The rest of the matrix elements

$$\langle 0|\mathcal{R}^{\mathrm{Lite,SYK}}_{K,R\to T}\left[\mathcal{N}^{\mathrm{SYK}}_{T\to K,R}[|1\rangle_T\langle 0|]\right]|1\rangle, \qquad \langle 1|\mathcal{R}^{\mathrm{Lite,SYK}}_{K,R\to T}\left[\mathcal{N}^{\mathrm{SYK}}_{T\to K,R}[|1\rangle_T\langle 1|]\right]|1\rangle$$

[14] The details of the calculation will be discussed in an upcoming paper [16].

are difficult to evaluate directly, as we will mention in footnote 17. In the next section, we evaluate these matrix elements indirectly from the results of this section.

Thus, to see the recovery (80), we need to study the behaviors of the matrix elements of $\mathcal{N}^\dagger\mathcal{N}$ which appear in the right-hand sides of Eqs. (81), (82), and (83). In order for the recovery to happen, these have to satisfy

$$\left\langle \hat{d}_{\tilde{L}} \right\rangle_\beta \cdot \langle 1|\mathcal{N}^{\mathrm{SYK}\dagger}_{K,R\to T}\left[\mathcal{N}^{\mathrm{SYK}}_{T\to K,R}\left[|0\rangle_T\langle 0|\right]\right]|1\rangle \overset{?}{\approx} 0, \tag{84}$$

$$\left\langle \hat{d}_{\tilde{L}} \right\rangle_\beta \cdot \langle 0|\mathcal{N}^{\mathrm{SYK}\dagger}_{K,R\to T}\left[\mathcal{N}^{\mathrm{SYK}}_{T\to K,R}\left[|0\rangle_T\langle 1|\right]\right]|1\rangle \overset{?}{\approx} 1. \tag{85}$$

We study the behaviors of the left-hand sides of Eqs. (84) and (85) below. To this end, it is convenient to rewrite the quantities as correlators. From the definitions of the channels in Eqs. (4) and (68), we obtain the left-left correlators

$$\begin{aligned}&\left\langle \hat{d}_{\tilde{L}} \right\rangle_\beta \cdot \langle 1|\mathcal{N}^{\mathrm{SYK}\dagger}_{K,R\to T}\left[\mathcal{N}^{\mathrm{SYK}}_{T\to K,R}\left[|0\rangle_T\langle 0|\right]\right]|1\rangle \\ &\quad = \frac{1}{Z_\delta}\cdot\frac{\left\langle \mathrm{TFD}\left|\psi_{i,L}(t-i\delta)\left(I_{\tilde{L}}\otimes\rho_{KR}\right)\psi_{i,L}(t+i\delta)\right|\mathrm{TFD}\right\rangle}{\mathrm{tr}_{KR}\left[(\rho_{KR})^2\right]},\end{aligned} \tag{86}$$

$$\begin{aligned}&\left\langle \hat{d}_{\tilde{L}} \right\rangle_\beta \cdot \langle 0|\mathcal{N}^{\mathrm{SYK}\dagger}_{K,R\to T}\left[\mathcal{N}^{\mathrm{SYK}}_{T\to K,R}\left[|0\rangle_T\langle 1|\right]\right]|1\rangle \\ &\quad = \frac{1}{Z_\delta}\cdot\frac{\left\langle \mathrm{TFD}\left|\psi_{i,L}(t-i\delta)\left(\rho_{\tilde{L}}\otimes I_{KR}\right)\psi_{i,L}(t+i\delta)\right|\mathrm{TFD}\right\rangle}{\mathrm{tr}_{KR}\left[(\rho_{KR})^2\right]},\end{aligned} \tag{87}$$

where the two fermions are put on the left system, and ρ_{KR} and $\rho_{\tilde{L}}$ are defined by

$$\rho_{\tilde{L}} = \mathrm{tr}_{KR}\left[|\mathrm{TFD}\rangle_{LR}\langle\mathrm{TFD}|\right], \qquad \rho_{KR} = \mathrm{tr}_{\tilde{L}}\left[|\mathrm{TFD}\rangle_{LR}\langle\mathrm{TFD}|\right]. \tag{88}$$

We give the derivation of the correlators in Appendix D.

We also note that the numerators in the above correlators can be written as

$$\begin{aligned}&\langle\mathrm{TFD}|\psi_{i,L}(t-i\delta)\left(I_{\tilde{L}}\otimes\rho_{KR}\right)\psi_{i,L}(t+i\delta)|\mathrm{TFD}\rangle \\ &\quad = \mathrm{tr}_{KR}\left[\mathrm{tr}_{\tilde{L}}\left[\psi_{i,L}(t+i\delta)\,|\mathrm{TFD}\rangle_{L,R}\langle\mathrm{TFD}|\,\psi_{i,L}(t-i\delta)^\dagger\right]\rho_{KR}\right]\end{aligned} \tag{89}$$

and

$$\begin{aligned}&\langle\mathrm{TFD}|\psi_{i,L}(t-i\delta)\left(\rho_{\tilde{L}}\otimes I_{KR}\right)\psi_{i,L}(t+i\delta)|\mathrm{TFD}\rangle \\ &\quad = \mathrm{tr}_{\tilde{L}}\left[\mathrm{tr}_{KR}\left[\psi_{i,L}(t+i\delta)\,|\mathrm{TFD}\rangle_{L,R}\langle\mathrm{TFD}|\,\psi_{i,L}(t-i\delta)^\dagger\right]\rho_{\tilde{L}}\right].\end{aligned} \tag{90}$$

These expressions are also useful for seeing that these quantities are related to "Renyi-2" quantities, as explained below.

Below, we would like to evaluate these correlators analytically, but the expressions in Eqs. (86) and (87) are not suitable for analytic treatment. This is because they are "specific site" correlators; thus, we cannot apply the large-N techniques to evaluate them. However, since we are basically interested in typical behaviors under highly chaotic dynamics in our setup, the specific choice of the embedding would *not* be essential. Therefore, below, we consider the "typical" embedding of the code information into the whole $\tilde{L}$ system uniformly. Therefore, we

replace these correlators with their averages on $\tilde{L}$,

$$\frac{1}{Z_\delta}\cdot\frac{\langle \mathrm{TFD}|\psi_{i,L}(t-i\delta)\ \left(I_{\tilde{L}}\otimes\rho_{KR}\right)\ \psi_{i,L}(t+i\delta)|\mathrm{TFD}\rangle}{\mathrm{tr}_{KR}\left[(\rho_{KR})^2\right]}$$

$$\to\frac{1}{N-K}\sum_{i=1}^{N-K}\frac{1}{Z_\delta}\cdot\frac{\langle \mathrm{TFD}|\psi_{i,L}(t-i\delta)\ \left(I_{\tilde{L}}\otimes\rho_{KR}\right)\ \psi_{i,L}(t+i\delta)|\mathrm{TFD}\rangle}{\mathrm{tr}_{KR}\left[(\rho_{KR})^2\right]} \tag{91}$$

and

$$\frac{1}{Z_\delta}\cdot\frac{\langle \mathrm{TFD}|\psi_{i,L}(t-i\delta)\ \left(\rho_{\tilde{L}}\otimes I_{KR}\right)\ \psi_{i,L}(t+i\delta)|\mathrm{TFD}\rangle}{\mathrm{tr}_{KR}\left[(\rho_{KR})^2\right]}$$

$$\to\frac{1}{N-K}\sum_{i=1}^{N-K}\frac{1}{Z_\delta}\cdot\frac{\langle \mathrm{TFD}|\psi_{i,L}(t-i\delta)\ \left(\rho_{\tilde{L}}\otimes I_{KR}\right)\ \psi_{i,L}(t+i\delta)|\mathrm{TFD}\rangle}{\mathrm{tr}_{KR}\left[(\rho_{KR})^2\right]}. \tag{92}$$

These replacements would change the correlators in subleading orders of N, but the essential physics would not be changed, because of typicality.

These averaged two-point functions are special cases of the (right-left) modular-flowed correlators of the form

$$\frac{1}{N-K}\sum_{i=1}^{N-K}\frac{\langle \mathrm{TFD}|\psi_{i,R}(\tau)\left(\rho_{\tilde{L}}^{n-1-k}\otimes\rho_{KR}^{k}\right)\psi_{i,L}(\tau')|\mathrm{TFD}\rangle}{\mathrm{tr}\left[\rho_{KR}^{n}\right]}, \tag{93}$$

where one of the fermions is put on the left system, and the other one is on the right system. In the Euclidean regime, they are computed by using the replica trick in Ref. [14] when $K\ll N$.

We use the result to compute "Rényi-2" (left-left) modular-flowed correlators (91,92) from the Euclidean (right-left) correlator (93), by taking the limits $k\to n-1$ (and $k\to 0$), and $n\to 2$, then analytically continuing to the Lorentzian regime. We note that there is a difference between the above correlator (Eq. (93)) computed in Ref. [14] and our correlators (Eqs. (91) and (92)), namely that in Eq. (93) two fermions are living on opposite sides but in our correlators they live on the same side. In our setup, one can relate the correlator to the diagrams in Fig. 7.

We study the correlators in the large-βJ limit because their analytic expressions are available in the limit. One can instead work in the large-q limit while keeping the value of βJ finite. We will not do this here because it is the former limit where the generalization to 2D conformal field theories (CFTs) is straightforward [16]. The right-hand sides of Eqs. (91) and (92) in the Euclidean regime are evaluated in the large βJ and $K\ll N$ limit as

$$\frac{1}{N-K}\sum_{i=1}^{N-K}\frac{\langle \mathrm{TFD}|\psi_{i,L}(\tau)\ \left(I_{\tilde{L}}\otimes\rho_{KR}\right)\ \psi_{i,L}(\tau')|\mathrm{TFD}\rangle}{\mathrm{tr}_{KR}\left[(\rho_{KR})^2\right]}$$

$$=G_{2\beta}(\tau+2\beta-\tau')+2\frac{K}{N}\left(\mathcal{F}(\tau+2\beta,\tau';\beta,0)-\mathcal{F}_0(\tau+2\beta,\tau';\beta,0)\right)+\mathcal{O}\left(\left(\frac{K}{N}\right)^2\right), \tag{94}$$

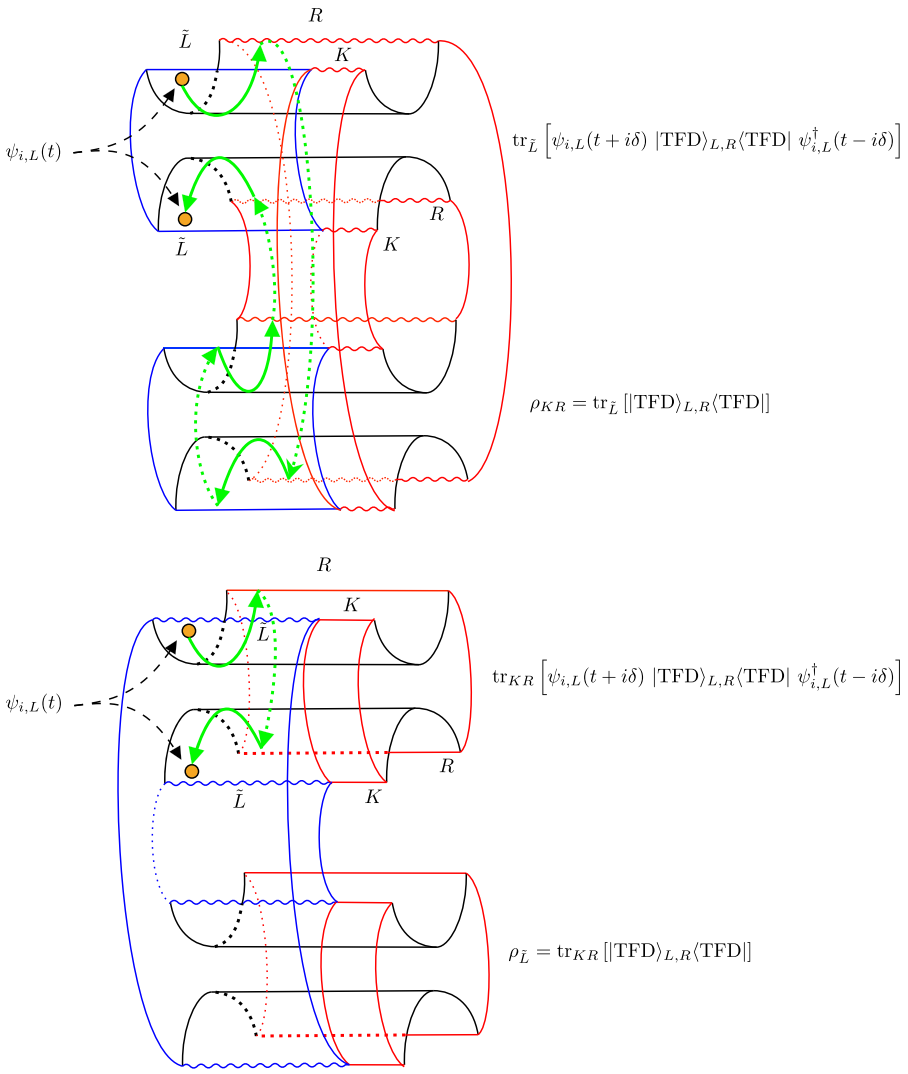

Fig. 7. Diagrams for the path integral calculation of the correlator (Eq. (86)) using the relation in Eq. (89) (top), and the other correlator (Eq. (87)) using Eq. (90) (bottom). The red regions in the figure correspond to subsystem RK, and the blue regions correspond to subsystem $\tilde{L}$. The semicircles correspond to the Euclidean segments that prepare the TFD states. Orange dots represent the insertions of the SYK Majorana fermion with the regularization, $\psi_{i,L}(t+i\delta)$. The combination of the upper two semicircles with the operator insertions corresponds to the density matrix $\mathrm{tr}_{\tilde{L}}[\psi_{i,L}\,|\mathrm{TFD}\rangle_{L,R}\langle\mathrm{TFD}|\,\psi^{\dagger}_{i,L}]$ (and $\mathrm{tr}_{KR}[\psi_{i,L}\,|\mathrm{TFD}\rangle_{L,R}\langle\mathrm{TFD}|\,\psi^{\dagger}_{i,L}]$), and the remaining combination represents the other one: ρ_{KR} (and $\rho_{\tilde{L}}$). Solid green arrows in the figure correspond to $\beta/2$ Euclidean evolutions. The two insertions are separated by Euclidean time 2β (top) and β (bottom). These separations are directly related to $\tau+2\beta$ and $\tau+\beta$ appearing in Eqs. (94) and (95), respectively.

$$\frac{1}{N-K}\sum_{i=1}^{N-K}\frac{\langle\mathrm{TFD}|\psi_{i,L}(\tau)\left(\rho_{\tilde{L}}\otimes I_{KR}\right)\psi_{i,L}(\tau')|\mathrm{TFD}\rangle}{\mathrm{tr}_{KR}\left[(\rho_{KR})^2\right]}$$

$$=G_{2\beta}(\tau+\beta-\tau')+2\frac{K}{N}\left(\mathcal{F}(\tau+\beta,\tau';\beta,0)-\mathcal{F}_0(\tau+\beta,\tau';\beta,0)\right)+\mathcal{O}\left(\left(\frac{K}{N}\right)^2\right). \tag{95}$$

Here, $G_{2\beta}(\tau)$ is a Euclidean thermal SYK two-point function for subsystem $\tilde{L}$ with periodicity 2β, and $\mathcal{F}(\tau_1, \tau_2; \tau_3, \tau_4)$ is the connected SYK four-point function, which is related to the bare one $\mathcal{F}_0(\tau_1, \tau_2; \tau_3, \tau_4)$ by the so-called ladder kernel $K_c(\tau_1, \tau_2; \tau_3, \tau_4)$,

$$\begin{aligned}
\mathcal{F}(\tau_1, \tau_2; \tau_3, \tau_4) &= \int d\tau \int d\tau' \frac{1}{1 - K_c(\tau_1, \tau_2; \tau, \tau')} \mathcal{F}_0(\tau, \tau'; \tau_3, \tau_4), \\
\mathcal{F}_0(\tau_1, \tau_2; \tau_3, \tau_4) &= G_{2\beta}(\tau_{13}) G_{2\beta}(\tau_{42}) - G_{2\beta}(\tau_{14}) G_{2\beta}(\tau_{32}), \qquad \tau_{ij} = \tau_i - \tau_j, \\
K_c(\tau_1, \tau_2; \tau_3, \tau_4) &= -J^2 (q-1) G_{2\beta}(\tau_{13}) G_{2\beta}(\tau_{24}) \left(G_{2\beta}(\tau_{34})\right)^{q-2}.
\end{aligned} \tag{96}$$

In the SYK model, these two-point and four-point functions are well-studied in many papers, e.g. Refs. [31,33–37]. See also Refs. [32,38] for the reviews and references therein.

The Euclidean times τ, τ' in Eqs. (94) and (95) are continued to the Lorentzian time with a regularization parameter $0 < \delta \ll 1$; $\tau \to -it - \delta$, $\tau' \to -it + \delta$. In this way, the correlator (94) is continued to Lorentzian time as an out-of-time ordering correlator (OTOC), $\tau_1 > \tau_3 > \tau_2 > \tau_4$, under the condition $1 \ll \beta J \ll N/K$. This correlator with the ordering is given by [31, 38],

$$\mathcal{F}(\tau_1, \tau_2; \tau_3, \tau_4) = G_{2\beta}(\tau_{12}) G_{2\beta}(\tau_{34}) \frac{2\beta J}{q^2 \pi C} \left[1 - \frac{\pi}{2} \frac{\sin\left(\frac{\pi}{\beta} \tau_{12;34}\right)}{\sin\left(\frac{\pi}{\beta} \cdot \frac{\tau_{12}}{2}\right) \sin\left(\frac{\pi}{\beta} \cdot \frac{\tau_{34}}{2}\right)} \right], \tag{97}$$

where $\tau_{12;\,34} = (\tau_1 + \tau_2)/2 - (\tau_3 + \tau_4)/2$, and C is a constant related to an overall constant of the Schwarzian action derived from the Schwinger–Dyson equation of the SYK model [31,38]. Thus, we have the following continuation:

$$\begin{aligned}
&\mathcal{F}(\tau + 2\beta, \tau'; \beta, 0) \to \mathcal{F}(-it - \delta + 2\beta, -it + \delta; \beta, 0) \\
&\qquad = 2 G_{2\beta}(2\beta - 2\delta) G_{2\beta}(\beta) \cdot \frac{2\beta J}{q^2 \pi C} \left[1 - \frac{\pi}{2} \frac{\cosh\left(\frac{\pi}{\beta} t\right)}{\sin\left(\frac{\pi \delta}{\beta}\right)} \right] \\
&\qquad \approx -2 G_{2\beta}(2\beta - 2\delta) G_{2\beta}(\beta) \cdot \frac{\beta J}{2q^2 C} \cdot \frac{\exp\left(\frac{\pi}{\beta} t\right)}{\sin\left(\frac{\pi \delta}{\beta}\right)}.
\end{aligned} \tag{98}$$

In particular, the correlator is exponentially growing in time. On the other hand, the other correlator (95) is continued to Lorentzian time with the ordering $\tau_3 > \tau_1 > \tau_2 > \tau_4$ under the condition $1 \ll \beta J \ll N/K$, therefore it is not OTOC. The correlator with the ordering $\tau_3 > \tau_1 > \tau_2 > \tau_4$ is given by

$$\begin{aligned}
\mathcal{F}(\tau_1, \tau_2; \tau_3, \tau_4) &= -G_{2\beta}(\tau_{12}) G_{2\beta}(\tau_{34}) \frac{2\beta J}{q^2 \pi C} \\
&\quad \times \left[\left(\frac{\pi \tau_{12}}{2\beta \tan\left(\frac{\pi}{\beta} \cdot \frac{\tau_{12}}{2}\right)} + \frac{\pi}{\tan\left(\frac{\pi}{\beta} \cdot \frac{\tau_{12}}{2}\right)} - 1 \right) \left(\frac{\pi \tau_{34}}{2\beta \tan\left(\frac{\pi}{\beta} \cdot \frac{\tau_{34}}{2}\right)} - 1 \right) \right],
\end{aligned} \tag{99}$$

and its analytic continuation is

$$\begin{aligned}\mathcal{F}(\tau+\beta,\tau';\beta,0)\to\mathcal{F}(-it-\delta+\beta,-it+\delta;\beta,0)\\ =-2G_{2\beta}(\beta-2\delta)G_{2\beta}(\beta)\cdot\frac{2\beta J}{q^2\pi C}\left[1-\left(\frac{\pi}{2}-\frac{\pi\delta}{\beta}\right)\tan\left(\frac{\pi\delta}{\beta}\right)\right].\end{aligned} \tag{100}$$

Clearly, this is time-independent, unlike the previous case.

We do not evaluate bare four-point functions $\mathcal{F}_0(\tau_1,\tau_2;\tau_3,\tau_4)$ for Eqs. (94) and (95), because they are particular combinations of the thermal SYK two-point functions with the power law behavior with respect to time, therefore they do not give dominant contributions to the correlators in Eqs. (94) and (95).

Combining the above results, we can obtain the analytic expressions of the quantities in Eqs. (94) and (95),

$$\begin{aligned}&\left\langle\hat{d}_{\tilde{L}}\right\rangle_\beta\cdot\langle 1|\mathcal{N}^{\mathrm{SYK}\dagger}_{K,R\to T}\left[\mathcal{N}^{\mathrm{SYK}}_{T\to K,R}\left[|0\rangle_T\langle 0|\right]\right]|1\rangle\\ &\approx\frac{1}{Z_\delta}\left[G_{2\beta}(2\beta-2\delta)-G_{2\beta}(2\beta-2\delta)G_{2\beta}(\beta)\cdot\frac{2\beta J}{q^2C}\cdot\frac{K}{N}\frac{\exp\left(\frac{\pi}{\beta}t\right)}{\sin\left(\frac{\pi\delta}{\beta}\right)}+\cdots\right]\\ &\approx\frac{G_{2\beta}(2\beta-2\delta)}{G_\beta(2\delta)}\left[1-\frac{G_{2\beta}(\beta)}{\sin\left(\frac{\pi\delta}{\beta}\right)}\cdot\frac{2\beta J}{q^2C}\cdot\frac{K}{N}\exp\left(\frac{\pi}{\beta}t\right)\right],\end{aligned} \tag{101}$$

and

$$\begin{aligned}&\left\langle\hat{d}_{\tilde{L}}\right\rangle_\beta\cdot\langle 0|\mathcal{N}^{\mathrm{SYK}\dagger}_{K,R\to T}\left[\mathcal{N}^{\mathrm{SYK}}_{T\to K,R}\left[|0\rangle_T\langle 1|\right]\right]|1\rangle\\ &\approx\frac{1}{Z_\delta}\left[G_{2\beta}(\beta-2\delta)-G_{2\beta}(\beta-2\delta)G_{2\beta}(\beta)\cdot\frac{8\beta J}{q^2\pi C}\cdot\frac{K}{N}\left[1-\left(\frac{\pi}{2}-\frac{\pi\delta}{\beta}\right)\tan\left(\frac{\pi\delta}{\beta}\right)\right]+\cdots\right]\\ &\approx\frac{G_{2\beta}(\beta-2\delta)}{G_\beta(2\delta)}\left[1-G_{2\beta}(\beta)\cdot\frac{8\beta J}{q^2\pi C}\cdot\frac{K}{N}\left[1-\left(\frac{\pi}{2}-\frac{\pi\delta}{\beta}\right)\tan\left(\frac{\pi\delta}{\beta}\right)\right]\right],\end{aligned} \tag{102}$$

where $\cdots$ includes bare four-point functions $\mathcal{F}_0(\tau_1,\tau_2;\tau_3,\tau_4)$, would-be subleading terms coming from the replacements (Eqs. (91) and (92)) in Eqs. (86) and (87), and the sub-subleading terms of the averaged correlators. In the final lines, we ignored them. These ignored terms do not change the essential physics of the discussions below. Thus, for the simplicity of the discussions below, we do not consider their contributions explicitly, but we need to keep in mind that these ignored terms include order-(K/N) contributions.

Let us consider the consequences of the above results. First, we focus on the ratios $G_{2\beta}(2\beta-2\delta)/G_\beta(2\delta)$ and $G_{2\beta}(\beta-2\delta)/G_\beta(2\delta)$ appearing in the above results. Since the SYK two-point function under the conformal limit $\beta J\gg 1$ is given by [31],

$$G_\beta(\tau)=b\left[\frac{\pi}{\beta\sin\frac{\pi\tau}{\beta}}\right]^{2\Delta},\qquad\Delta=\frac{1}{q},\quad J^2b^q\pi=\left(\frac{1}{2}-\Delta\right)\tan\pi\Delta, \tag{103}$$

we can evaluate the ratios as follows:

$$\frac{G_{2\beta}(2\beta-2\delta)}{G_\beta(2\delta)}=\cos^{2\Delta}\left(\frac{\pi\delta}{\beta}\right), \tag{104}$$

and

$$\frac{G_{2\beta}(\beta-2\delta)}{G_\beta(2\delta)}=\sin^{2\Delta}\left(\frac{\pi\delta}{\beta}\right). \tag{105}$$

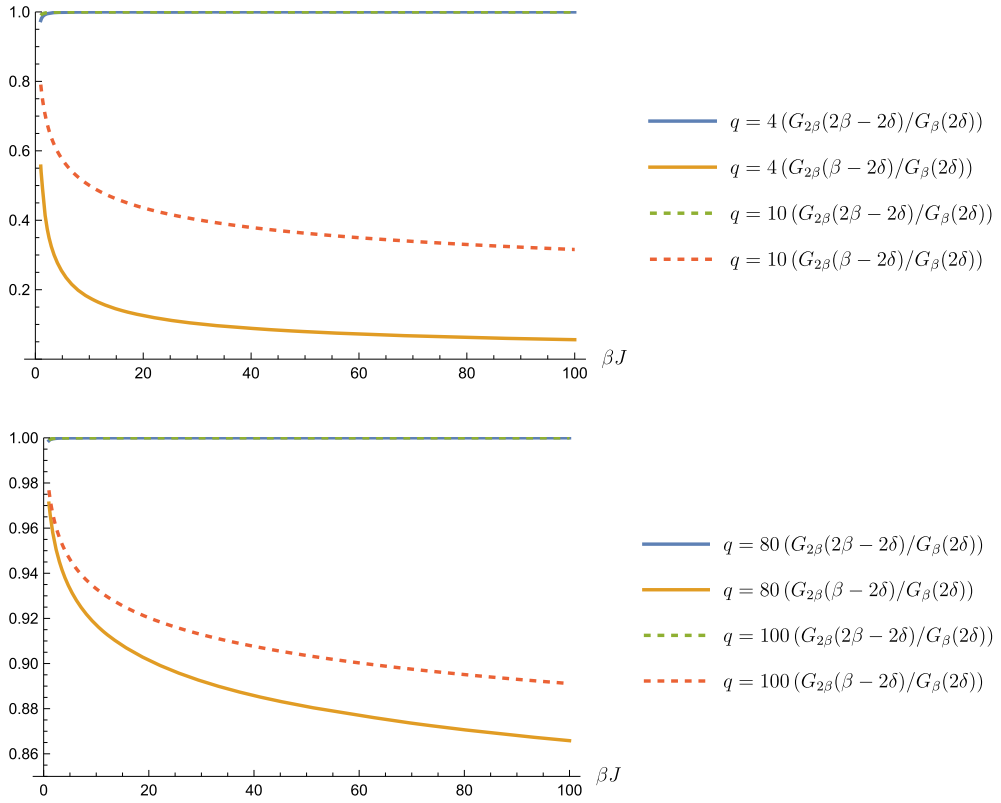

Fig. 8. Plots of the ratios in Eqs. (104) and (105) as a function of βJ for smaller q (top), and for larger q (bottom). Here, we set $\delta J = 0.1$. For large-q regions, all the ratios become close to 1.

Thus, these ratios cannot be 1 simultaneously for general δ and β. However, since $\Delta = 1/q$ when q is large, these ratios are close to 1. We give plots of the above two functions for several q in Fig. 8. As we can see from the plots in Fig. 8 or directly from Eqs. (104) and (105), we need to consider a (relatively) large-q regime, which implies that the SYK Majorana fermion has a small conformal dimension, $\Delta = 1/q \ll 1$, in order to achieve recovery.

One may wonder why here we take the large-q limit, because the $(\text{SYK})_q$ is chaotic for all $q \geq 4$, thus the identities Eqs. (84) and (85) are expected to hold for any value of q in this range. Nevertheless, here we have to take the large-q limit because we define the code subspace using the SYK Majorana fermion operator $\psi_{i,L}$ and the calculations of the relevant correlation functions are possible only in the large-βJ limit where the entanglement between L and R is weak. Because of the weakness of the entanglement, the recovery is only possible when the dimension of the operator that defines the code subspace is small, implying the necessity of taking the large-q limit.

Next, we consider the two-point function $G_{2\beta}(\beta)$ appearing in the subleading terms. The two-point function $G_{2\beta}(\beta)$ can be written as

$$G_{2\beta}(\beta) = b\left[\frac{\pi}{2\beta \sin\frac{\pi}{2}}\right]^{2\Delta} = \left[\left(\frac{1}{2} - \Delta\right)\frac{\pi \tan \pi\Delta}{(2\beta J)^2}\right]^{\Delta}. \tag{106}$$

The above expression includes $(1/\beta J)^{\Delta}$, thus in the $\beta J \to \infty$ limit, the SYK two-point function $G_{2\beta}(\beta)$ vanishes. We also note the q-dependence of the SYK two-point function. Plots of the above function and $\beta J G_{2\beta}(\beta)$ for several $q = \Delta^{-1}$ are given in Figs. 9 and 10, respectively. The plots show that as q increases, the two-point functions $G_{2\beta}(\beta)$ and $\beta J G_{2\beta}(\beta)$ take larger values.

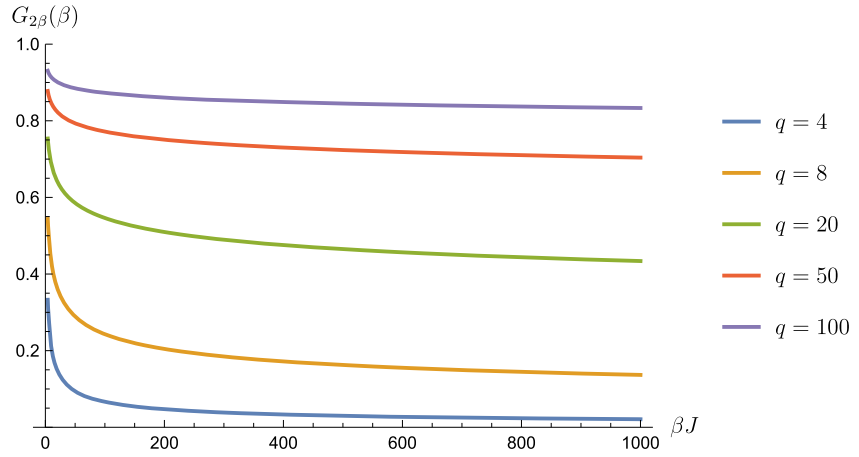

Fig. 9. Plots of the SYK two-point function $G_{2\beta}(\beta)$, Eq. (106), as a function of βJ for several $q = \Delta^{-1}$.

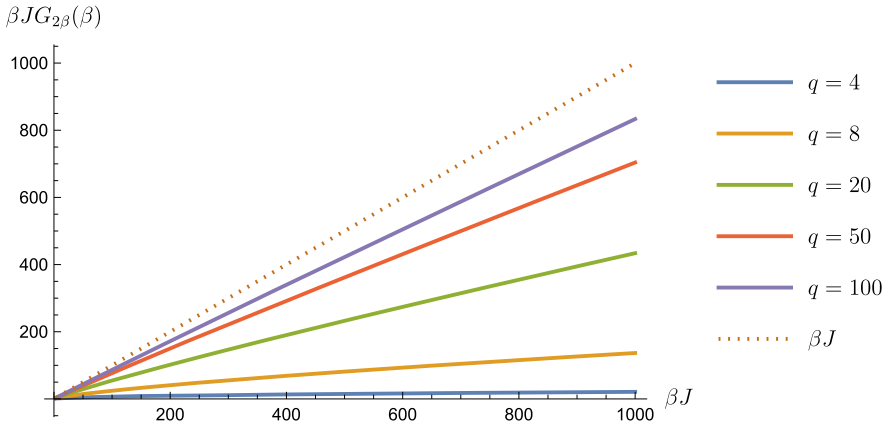

Fig. 10. Plots of $\beta J G_{2\beta}(\beta)$ as a function of βJ for several $q = \Delta^{-1}$. The dotted line is just βJ, which is equivalent to $\beta J G_{2\beta}(\beta)$ under the $q \to \infty$ limit.

Thus, from the above discussion, in the strict $\beta J \to \infty$ limit,[15] we have $G_{2\beta}(\beta) \to 0$, hence the second terms including $G_{2\beta}(\beta)$ in Eqs. (101) and (102) vanish if we keep the exponential factor $\exp(\pi t/\beta)$ in Eq. (101) fixed. Therefore, in this strict $\beta J \to \infty$ limit, we cannot have contributions from the second terms including $G_{2\beta}(\beta)$ in Eqs. (101) and (102). These terms are of order K/N and crucial for the following discussion.

Finally, let us focus on the time dependence of the results in Eqs. (101) and (102). First, we focus on the second case (102). This result is time-independent at least up to the K/N-order, and the second term is always suppressed by the time-independent factor at the K/N-order, thus the second term is very small compared with the first term. This implies that the quantity (102) is almost given by the ratio $G_{2\beta}(\beta - 2\delta)/G_{\beta}(2\delta)$, which becomes close to 1 when q is large.

Next, we focus on Eq. (101). Because of the exponential time-dependent factor, this correlator has crucially different behavior as a function of time from Eq. (102). For early times $t \ll 1$, the

[15] We note that to consider the perturbative expansion, we have assumed $\beta J \ll N/K$, and also implicitly assumed $q \ll N/K$ for large q. Thus, we cannot take the $\beta J \to \infty$ or $q \to \infty$ limits, unless we take the $N/K \to \infty$ limit. However, the limit $N/K \to \infty$ implies that there is almost no Hawking radiation compared to the entire Hawking radiation $K/N \to 0$. Intuitively, in such a situation, we would not be able to recover the diary information from the Hawking radiation.

exponential in the second term can be approximated by 1, they are similar. However, because of the exponentially growing factor, the perturbative expansion with respect to K/N breaks down, similar to the fact that the perturbative calculations of OTOCs in $1/N$ become invalid. The time scale of this breakdown can be estimated by equating the second term with the first term in Eq. (101). From the condition, we can find a critical time t_*,[16]

$$\frac{K}{N}\exp\left(\frac{\pi}{\beta}t_*\right)\sim 1 \qquad \Longrightarrow \quad t_* = \frac{\beta}{\pi}\log\left(\frac{N}{K}\right) = 2t_{\text{Scram}}, \tag{107}$$

where we introduce the usual scrambling time t_{Scram} [39] given by

$$t_{\text{Scram}} = \frac{\beta}{2\pi}\log\left(\frac{N}{K}\right). \tag{108}$$

Using this time scale, we can rewrite the correlator (101) as

$$\begin{aligned}&\left\langle \hat{d}_{\tilde{L}}\right\rangle_\beta \cdot \langle 1|\mathcal{N}^{\text{SYK}\dagger}_{K,R\to T}\left[\mathcal{N}^{\text{SYK}}_{T\to K,R}\left[|0\rangle_T\langle 0|\right]\right]|1\rangle \\ &\approx \frac{G_{2\beta}(2\beta-2\delta)}{G_\beta(2\delta)}\left[1-\frac{G_{2\beta}(\beta)}{\sin\left(\frac{\pi\delta}{\beta}\right)}\cdot\frac{2\beta J}{q^2C}\cdot\exp\left(\frac{\lambda_L}{2}\left(t-2t_{\text{Scram}}\right)\right)\right],\end{aligned} \tag{109}$$

where we introduce the Lyapunov exponent λ_L for a black hole with temperature β,

$$\lambda_L = \frac{2\pi}{\beta}. \tag{110}$$

Thus, around the critical time, which is twice the scrambling time, we can see that the overall coefficient of $G_{2\beta}(2\beta-2\delta)/G_{2\beta}(2\delta)$ becomes very small as usual for OTOC correlators. This reproduces the expected result (84) under the condition $\beta J \gg 1$.

From the discussion so far, we have confirmed that the matrix elements (Eqs. (81), (82), and (83)) do behave as we expect them to under the condition $1 \ll \beta J \ll N/K$.

5. Expected properties of the Petz-lite under the SYK dynamics

So far, we have confirmed that the matrix elements we computed (84,85) reproduce our expected results under the conditions of relatively large-q interaction, after the critical time $t_* = 2t_{\text{Scram}}$. Additionally, of course, the following trivial matrix element is equal to 1 by the definition,

$$\left\langle \hat{d}_{\tilde{L}}\right\rangle_\beta \cdot \langle 0|\mathcal{N}^{\text{SYK}\dagger}_{K,R\to T}\left[\mathcal{N}^{\text{SYK}}_{T\to K,R}\left[|0\rangle_T\langle 0|\right]\right]|0\rangle = 1. \tag{111}$$

Also, we can obtain the same consequences for two related matrix elements. Let us explain them. First, the matrix element Eq. (84), which becomes close to 0, is directly related to

$$\left\langle \hat{d}_{\tilde{L}}\right\rangle_\beta \cdot \langle 1|\mathcal{N}^{\text{SYK}\dagger}_{K,R\to T}\left[\mathcal{N}^{\text{SYK}}_{T\to K,R}[|0\rangle_T\langle 0|]\right]|1\rangle = \left\langle \hat{d}_{\tilde{L}}\right\rangle_\beta \cdot \langle 0|\mathcal{N}^{\text{SYK}\dagger}_{K,R\to T}\left[\mathcal{N}^{\text{SYK}}_{T\to K,R}[|1\rangle_T\langle 1|]\right]|0\rangle \tag{112}$$

via the definition of the adjoint channel (8). Thus, this matrix element also becomes close to 0 after the critical time, and the behavior is consistent with our expectation.

[16] In defining the critical time, we might have ambiguity as to which factors should be included in the critical time (or correspondingly the scrambling time), e.g. βJ and also $G_{2\beta}(\beta)$. However, as we saw before, the two-point function is typically order one $G_{2\beta}(\beta) = \mathcal{O}(1)$, thus we might not need to include the factor in the scrambling time. Another factor, $1/\sin\left(\frac{\pi\delta}{\beta}\right)$, can be set to be $\mathcal{O}(1)$ by setting the cutoff δ suitably. For the other factor βJ, since we have the condition $\beta J \ll N/K$, the factor cannot give a significant contribution compared to the leading factor N/K; thus, including the factor would be redundant. Therefore, the critical time here would be the simplest choice.

Next, for the matrix element Eq. (85), being almost equal to 1, we have the following relation through the definition of the adjoint channel (8) again,

$$\left\langle \hat{d}_{\tilde{L}} \right\rangle_\beta \cdot \langle 0|\mathcal{N}^{\mathrm{SYK}\dagger}_{K,R\to T}\left[\mathcal{N}^{\mathrm{SYK}}_{T\to K,R}[|0\rangle_T\langle 1|]\right]|1\rangle = \left\langle \hat{d}_{\tilde{L}} \right\rangle_\beta \cdot \langle 1|\mathcal{N}^{\mathrm{SYK}\dagger}_{K,R\to T}\left[\mathcal{N}^{\mathrm{SYK}}_{T\to K,R}[|1\rangle_T\langle 0|]\right]|0\rangle\,. \tag{113}$$

Thus, although we have eight nontrivial matrix elements (80) that should be checked, we already know the behavior of the above five matrix elements, and there are still three matrix elements remaining. However, since two of them are related by complex conjugation, essentially we need to investigate the following two matrix elements:

$$\left\langle \hat{d}_{\tilde{L}} \right\rangle_\beta \cdot \langle 0|\mathcal{N}^{\mathrm{SYK}\dagger}_{K,R\to T}\left[\mathcal{N}^{\mathrm{SYK}}_{T\to K,R}[|1\rangle_T\langle 0|]\right]|1\rangle, \tag{114}$$

and

$$\left\langle \hat{d}_{\tilde{L}} \right\rangle_\beta \cdot \langle 1|\mathcal{N}^{\mathrm{SYK}\dagger}_{K,R\to T}\left[\mathcal{N}^{\mathrm{SYK}}_{T\to K,R}[|1\rangle_T\langle 1|]\right]|1\rangle. \tag{115}$$

Here, the first matrix element is related to the following one:

$$\left(\left\langle \hat{d}_{\tilde{L}} \right\rangle_\beta \cdot \langle 0|\mathcal{N}^{\mathrm{SYK}\dagger}_{K,R\to T}\left[\mathcal{N}^{\mathrm{SYK}}_{T\to K,R}[|1\rangle_T\langle 0|]\right]|1\rangle\right)^* = \left\langle \hat{d}_{\tilde{L}} \right\rangle_\beta \cdot \langle 1|\mathcal{N}^{\mathrm{SYK}\dagger}_{K,R\to T}\left[\mathcal{N}^{\mathrm{SYK}}_{T\to K,R}[|0\rangle_T\langle 1|]\right]|0\rangle\,. \tag{116}$$

In evaluating these matrix elements, we cannot directly use the technique of Ref. [14], unlike the cases for the matrix elements in Eqs. (86) and (87).[17] In an upcoming paper [16], we will report their results, but here we explain their expected behaviors from our obtained results. To this end, it would be useful to introduce the Kraus representation of the quantum channel (67),

$$\mathcal{N}^{\mathrm{SYK}}_{T\to K,R}[\rho_T] = \sum_{m=1}^{d_{\tilde{L}}} E^{\mathrm{SYK}}_m \rho_T E^{\mathrm{SYK}\dagger}_m \tag{117}$$

where E^{SYK}_m is the Kraus operator given by

$$E^{\mathrm{SYK}}_m = {}_{\tilde{L}}\langle m|\, U_L V_{T,L\to L}\, |\mathrm{TFD}\rangle_{L,R}\,. \tag{118}$$

We can obtain this Kraus representation by introducing an orthonormal basis of the subsystem $\tilde{L}$ as $\left\{|m\rangle_{\tilde{L}}\right\}_{m=1}^{d_{\tilde{L}}}$. We also note that the adjoint channel (68) can be written as

$$\mathcal{N}^{\mathrm{SYK}\dagger}_{K,R\to T}[\mathcal{O}_{KR}] = \sum_{m=1}^{d_{\tilde{L}}} E^{\mathrm{SYK}\dagger}_m \mathcal{O}_{KR} E^{\mathrm{SYK}}_m. \tag{119}$$

Using this Kraus representation, it is possible to extract the very important "typical" relation from our results. Here, "typical" means that the relation almost does not depend on the detail of a specific state $|m\rangle_{\tilde{L}}$ in the subsystem $\tilde{L}$, corresponding to a black hole microstate. First, the

[17] We briefly explain the reason why the evaluations of the matrix elements Eqs. (115) and (116) are difficult. The reason is that they do not have simple expressions like Eqs. (89) and (90) naively. Of course, for matrix element Eq. (115), we can consider a similar expression like Eq. (89) if replacing the TFD state with the excited state $\psi_{i,L}\,|\mathrm{TFD}\rangle_{L,R}$, but in that case, we can no longer use the techniques in Ref. [14], and we need to consider the modular operator for the excited state. For the other matrix element (116), we naively need to introduce transition matrices, not density matrices, to write it in terms of a correlator.

matrix element in Eq. (111) is equal to 1 and can be expressed as

$$\begin{aligned}
&\left\langle \hat{d}_{\tilde{L}} \right\rangle_\beta \cdot \langle 0| \mathcal{N}^{\mathrm{SYK}\dagger}_{K,R\to T} \left[\mathcal{N}^{\mathrm{SYK}}_{T\to K,R} \left[|0\rangle_T \langle 0| \right] \right] |0\rangle \\
&= \left\langle \hat{d}_{\tilde{L}} \right\rangle_\beta \sum_{m,n=1}^{d_{\tilde{L}}} {}_T\left\langle 0 \left| E^{\mathrm{SYK}\dagger}_m E^{\mathrm{SYK}}_n \right| 0 \right\rangle_T \left\langle 0 \left| E^{\mathrm{SYK}}_n E^{\mathrm{SYK}\dagger}_m \right| 0 \right\rangle_T \\
&= \left\langle \hat{d}_{\tilde{L}} \right\rangle_\beta \sum_{m,n=1}^{d_{\tilde{L}}} \left| {}_T\left\langle 0 \left| E^{\mathrm{SYK}\dagger}_m E^{\mathrm{SYK}}_n \right| 0 \right\rangle_T \right|^2 ,
\end{aligned} \tag{120}$$

and we expect the typical relation

$$ {}_T\langle 0| E^{\mathrm{SYK}\dagger}_m E^{\mathrm{SYK}}_n |0\rangle_T \sim \frac{1}{\sqrt{d_{\tilde{L}} \cdot \left\langle \hat{d}_{\tilde{L}} \right\rangle_\beta}} \delta_{mn}. \tag{121}$$

Next, we focus on the matrix element in Eq. (85). This matrix element is also equal to 1, and we can express the matrix element in terms of the Kraus operators,

$$\begin{aligned}
&\left\langle \hat{d}_{\tilde{L}} \right\rangle_\beta \cdot \langle 0| \mathcal{N}^{\mathrm{SYK}\dagger}_{K,R\to T} \left[\mathcal{N}^{\mathrm{SYK}}_{T\to K,R} \left[|0\rangle_T \langle 1| \right] \right] |1\rangle \\
&= \left\langle \hat{d}_{\tilde{L}} \right\rangle_\beta \sum_{m,n=1}^{d_{\tilde{L}}} {}_T\left\langle 0 \left| E^{\mathrm{SYK}\dagger}_m E^{\mathrm{SYK}}_n \right| 0 \right\rangle_T \left\langle 1 \left| E^{\mathrm{SYK}}_n E^{\mathrm{SYK}\dagger}_m \right| 1 \right\rangle_T .
\end{aligned} \tag{122}$$

By using the relation in Eq. (121), we extract a similar relation,

$$ {}_T\langle 1| E^{\mathrm{SYK}\dagger}_m E^{\mathrm{SYK}}_n |1\rangle_T \sim \frac{1}{\sqrt{d_{\tilde{L}} \cdot \left\langle \hat{d}_{\tilde{L}} \right\rangle_\beta}} \delta_{mn}. \tag{123}$$

Finally, the time-dependent matrix element (Eq. (84)), which almost vanishes around the critical time t_*, can be written as

$$\begin{aligned}
&\left\langle \hat{d}_{\tilde{L}} \right\rangle_\beta \cdot \langle 1| \mathcal{N}^{\mathrm{SYK}\dagger}_{K,R\to T} \left[\mathcal{N}^{\mathrm{SYK}}_{T\to K,R} \left[|0\rangle_T \langle 0| \right] \right] |1\rangle \\
&= \left\langle \hat{d}_{\tilde{L}} \right\rangle_\beta \sum_{m,n=1}^{d_{\tilde{L}}} {}_T\left\langle 1 \left| E^{\mathrm{SYK}\dagger}_m E^{\mathrm{SYK}}_n \right| 0 \right\rangle_T \left\langle 0 \left| E^{\mathrm{SYK}}_n E^{\mathrm{SYK}\dagger}_m \right| 1 \right\rangle_T \\
&= \left\langle \hat{d}_{\tilde{L}} \right\rangle_\beta \sum_{m,n=1}^{d_L} \left| {}_T\left\langle 1 \left| E^{\mathrm{SYK}\dagger}_m E^{\mathrm{SYK}}_n \right| 0 \right\rangle_T \right|^2 .
\end{aligned} \tag{124}$$

From this expression, we expect the following relation and its complex conjugation,

$$ {}_T\langle 1| E^{\mathrm{SYK}\dagger}_m E^{\mathrm{SYK}}_n |0\rangle_T \sim 0, \tag{125}$$

around and after the critical time.

Combining the above expectations, we obtain the typically expected relation[18]

$$ {}_T\left\langle T \left| E^{\mathrm{SYK}\dagger}_m E^{\mathrm{SYK}}_n \right| T' \right\rangle_T \sim \frac{1}{\sqrt{d_{\tilde{L}} \cdot \left\langle \hat{d}_{\tilde{L}} \right\rangle_\beta}} \delta_{mn} \delta_{TT'} \qquad \text{for } t \gtrsim t_*, \tag{126}$$

[18]Here, we check the Knill–Laflamme condition from our obtained results. However, in principle, it would be possible to investigate the Knill–Laflamme condition directly by introducing a basis [30]. It would be interesting to investigate this topic.

which corresponds to the Knill–Laflamme condition [40].

Using this relation, the remaining matrix elements (Eqs. (114) and (115)) are expected to behave as follows:

$$\left\langle \hat{d}_{\tilde{L}} \right\rangle_\beta \cdot \langle 0|\mathcal{N}^{\mathrm{SYK}\dagger}_{K,R\to T}\left[\mathcal{N}^{\mathrm{SYK}}_{T\to K,R}\left[|1\rangle_T\langle 0|\right]\right]|1\rangle = \left\langle \hat{d}_{\tilde{L}} \right\rangle_\beta \sum_{m,n=1}^{d_L} {}_T\langle 0\left|E^{\mathrm{SYK}\dagger}_m E^{\mathrm{SYK}}_n\right|1\rangle_T \langle 0\left|E^{\mathrm{SYK}}_n E^{\mathrm{SYK}}_m\right|1\rangle_T \tag{127}$$

$$\sim 0 \quad \text{for } t \gtrsim t_*,$$

and

$$\left\langle \hat{d}_{\tilde{L}} \right\rangle_\beta \cdot \langle 1|\mathcal{N}^{\mathrm{SYK}\dagger}_{K,R\to T}\left[\mathcal{N}^{\mathrm{SYK}}_{T\to K,R}\left[|1\rangle_T\langle 1|\right]\right]|1\rangle = \left\langle \hat{d}_{\tilde{L}} \right\rangle_\beta \sum_{m,n=1}^{d_L} {}_T\langle 1\left|E^{\mathrm{SYK}\dagger}_m E^{\mathrm{SYK}}_n\right|1\rangle_T \langle 1\left|E^{\mathrm{SYK}}_n E^{\mathrm{SYK}\dagger}_m\right|1\rangle_T \tag{128}$$

$$\sim 1$$

These results are, of course, consistent with our original expectation (80), but the discussion so far using the typical relation is indirect (126). Nevertheless, since this typicality is strong enough for a highly chaotic theory, we expect that nearly identical results can be obtained by direct calculations of the matrix elements (114,115).

6. Discussion

In this paper, we studied a recovery map for the HP-type scrambling channel $\mathcal{N}$. We showed that one can use a simplified recovery map, called Petz-lite, consisting of the adjoint channel $\mathcal{N}^\dagger$ with a suitable normalization factor. We considered two examples, the HP setup and the SYK model, and showed that in both cases, the Petz-lite indeed works as a recovery map. Also, we found that if the Petz-lite for the SYK case is used to recover information of a given code subspace, it takes twice the scrambling time for the recovery. However, in the SYK model case, we did not evaluate all of the matrix elements necessary to show the recovery because of technical difficulties. Instead, we indirectly evaluated them in Sect. 5. In an upcoming paper [16] we will explain their results, and also some generalizations of our results.

Let us discuss our results. First, we focus on the physical interpretation of the critical time given by twice the scrambling time, $t_* = 2t_{\mathrm{Scram}}$, when the matrix elements give the input information, $\mathcal{R}[\mathcal{N}[\rho]] \sim \rho$. It was argued in Ref. [39] that information of a diary thrown into a black hole appears after the scrambling time. This means that, after the scrambling time, the HP scrambling channel $\mathcal{N}$ maps the diary information to Hawking radiation completely. However, even if the diary information appears in the Hawking radiation, it is difficult to get it directly since the information is uniformly embedded into the Hawking radiation. To extract the information, we need a recovery operation given by the Petz-lite $\mathcal{R} \sim \mathcal{N}^\dagger$. Since it is the adjoint of the HP channel $\mathcal{N}$, it again takes the scrambling time to apply the recovery map. Thus, in total, we need to wait for twice the scrambling time for the identity (80) to be satisfied.

Next, let us explain the bulk interpretation of our results.[19] The bulk interpretation comes from the island prescription [1,2]. First, the HP setup concerns post-Page time regimes. In these regimes, there is an island, which is a nontrivial entanglement wedge of Hawking radiation in

[19] We note that since currently there is no clear understanding of a dual gravitational theory for a subset of the SYK Majorana fermions (or Majorana spin chain), we cannot check the interpretation using the gravity side explicitly, at least in the context of $\mathrm{NAdS}_2/\mathrm{NCFT}_1$. However, there are several proposals for such a gravitational treatment, e.g. in Ref. [14]. One would be able to use them to check the bulk interpretation.

the black hole interior. Thus, if one throws a diary into a black hole and waits for the scrambling time, then the diary enters the island region, implying that the diary is encoded into the Hawking radiation in a very complicated way. The mechanism by which the thrown diary is encoded into the Hawking radiation corresponds to our quantum channel $\mathcal{N}$. To recover the diary information from the Hawking radiation, we need to consider the recovery operation corresponding to the map $\mathcal{R} \sim \mathcal{N}^\dagger$. The recovery map is given by the adjoint channel of the quantum channel $\mathcal{N}$. In the bulk side, the action of the adjoint channel $\mathcal{N}^\dagger$ means the "reverse" process of the original quantum channel $\mathcal{N}$.[20] More precisely, the "reverse" process is given as follows: First, we start from the output state provided by the action of the quantum channel $\mathcal{N}$, implying the diary is located on the island at some time slice Σ. The application of the adjoint channel $\mathcal{N}^\dagger$ is then interpreted as replacing the future of this time slice Σ by a white hole. Because of the replacement, the diary on the island region of the original black hole is coming out from the horizon of the white hole. Here, the reason why the white hole appears is that the adjoint channel includes the Hermitian conjugation of unitaries U (and $U^\dagger$) compared to the quantum channel $\mathcal{N}$. Thus, the diary thrown into the black hole reappears from the white hole induced by $\mathcal{N}^\dagger$. This bulk interpretation is consistent with the critical time. This is because, after throwing the diary, it takes the scrambling time for the diary to enter the island region, and in the "reverse" process, it would also take the scrambling time for the diary to go outside the island region and the horizon.

Finally, we end by discussing some of our in-progress works and future directions.

Analysis in high-temperature regime, $\beta J \ll 1$. In this paper, we have focused on the large-βJ limit (low-temperature limit) in the SYK model to make the calculation analytic and for the purpose of the generalization to a 2D CFT case. In the limit, we can use emergent conformal symmetry of the SYK model, and also we would be able to use semiclassical intuition of the dual Jackiw–Teitelboim gravity, but we have a relatively weak initial entangled state $|\mathrm{TFD}\rangle_{L,R}$ between the left and right SYK systems. Due to this weak entangled state, we would require some conditions to consider a successful recovery protocol, e.g. a large-q regime. Thus, analysis without taking the large-βJ limit would be interesting. In that case, we would need to consider numerical approaches.

Direct bulk analysis and relation to other protocols. In this paper, we studied the recovery protocol from the boundary CFT perspective. One would be able to consider corresponding bulk computations. Also, it would be interesting to figure out the relation between other proposed protocols, e.g. Refs. [41–44] and ours.[21]

Generalization to (holographic) CFT_2 and other systems. While this paper focuses on the SYK model, which is a $0+1$-dimensional quantum system, it can also be interpreted as a spin chain with q-body SYK interactions. Thus, we can interpret that the SYK model has a spatial direction effectively. As a result, we expect that a similar analysis can be applied to a 2D CFT exhibiting chaos, e.g. a 2D holographic CFT. Indeed, one of the HP setups in a 2D holographic CFT is introduced in Ref. [29].

[20] Here, we note that in these two processes, we need to use two different (remaining) black holes since, in defining the quantum channel, (remaining) black holes are treated as internal degrees of freedom of the quantum channel.

[21] For such protocols, one can characterize protocol by computing "price," "distance," etc. as in Refs. [14,45,46]. One would be able to find the relation between our results and such quantities.

Also, there are further possibilities for generalizations to other systems exhibiting chaos. For example, studying the Petz-lite in a chaotic spin chain would be interesting.

Chaotic–integrable transition. In this paper, the chaotic nature is important for the simplification of the Petz map to the Petz-lite. Thus, if a system does not exhibit a chaotic nature (in other words, the system is integrable), then the Petz-lite (also the original Petz map) is not expected to work correctly. This is because, in an integrable system, the decoupling condition is not expected to hold. In the framework of the SYK model, we can prepare integrable and non-integrable (chaotic) situations by adding two-body interaction [47]. Using the setup, we would be able to study the Petz-lite.

Higher-dimensional code subspace? The SYK version of the HP setup studied in this paper treats the 2D code subspace spanned by the vacuum and the excited state. However, in a more realistic situation, one needs to deal with code subspaces with dimensions greater than two. For example, when the interior of a black hole is viewed as a code subspace embedded into the Hawking radiation, the dimension of its Hilbert space has to be large enough to accommodate a part of the semiclassical quantum field theory degrees of freedom to have a geometric interpretation of the black hole interior.[22] To this end, one would need to consider a more complicated embedding involving, e.g. states like $\psi_{i,L}\psi_{j\neq i,L}\left|\mathrm{TFD}\right\rangle_{L,R}$. In that case, we can evaluate corresponding matrix elements in principle, but it would be difficult to evaluate them analytically since we encounter higher-point functions.

Another possibility for higher-dimensional code subspace is to consider a random embedding and the double-scaling limit. For example, we might be able to use the state $\kappa_{ij}\psi_{i,L}\psi_{j,L}\left|\mathrm{TFD}\right\rangle_{L,R}$, where κ_{ij} is random like observables in the double-scaled SYK model [49]. In this case, by taking the double-scaling limit and using chord diagram techniques, we might be able to evaluate the resulting matrix elements analytically. Also, this might open up an interesting connection between QEC in the SYK model and recent discussions of the von Neumann algebra of quantum gravity, in particular, Ref. [50].

Acknowledgements

We thank Yoshifumi Nakata for discussions. A.M. thanks Norihiro Iizuka, Tomoki Nosaka, Masahiro Nozaki, and Jia Tian for comments. A.M. also thanks Chen Bai for related discussions. A.M. thanks the workshop "Beijing Osaka String/Gravity/Black Hole Workshop" at Kavli Institute for Theoretical Sciences (KITS), where this work was presented. A.M. also thanks the long-term workshop "Quantum Information, Quantum Matter and Quantum Gravity" YITP-T-23-01 at Yukawa Institute for Theoretical Physics (YITP), where this work was also presented. Y.N. was supported by Japan Science and Technology Agency (JST), the establishment of university fellowships towards the creation of science technology innovation, Grant Number JPMJFS2123. T.U. was supported in part by Japan Society for the Promotion of Science (JSPS) Grant-in-Aid for Young Scientists 19K14716 and in part by Ministry of Education, Culture, Sports, Science and Technology (MEXT) KAKENHI Grant-in-Aid for Transformative Research Areas A "Extreme Universe" No. 21H05184.

Funding

Open Access funding: SCOAP[3].

[22]Of course, the interior degrees of freedom may appear to be infinite, but almost all of them cannot contribute due to postselection [48]. Even in that case, there can be degrees of freedom with Bekenstein–Hawking entropy.

Appendix A. Derivation of the Petz-lite using the Kraus representation

In this appendix, we derive the Petz-lite with a different normalization factor based on Ref. [51]. See, e.g. Sect. 10.3 of Ref. [52] for related reviews.

We start with the Kraus representation of the HP channel (4). The Kraus representation can be introduced by expressing the trace as

$$\begin{aligned}\mathcal{N}_{T\to D,B}[\rho_T] &= \mathrm{tr}_C\left[(U_{T,A\to C,D}\otimes I_B)(\rho_T\otimes|\mathrm{EPR}\rangle_{A,B}\langle\mathrm{EPR}|)(U^\dagger_{T,A\to C,D}\otimes I_B)\right]\\ &= \sum_{m=1}^{d_C} {}_C\langle m|(U_{T,A\to C,D}\otimes I_B)\,|\mathrm{EPR}\rangle_{A,B}\;\rho_{T\;A,B}\,\langle\mathrm{EPR}|\,(U^\dagger_{T,A\to C,D}\otimes I_B)|m\rangle_C\\ &= \sum_{m=1}^{d_C} E_m\rho_T E_m^\dagger,\end{aligned} \tag{A1}$$

where $|m\rangle_C$ is an orthonormal basis of subsystem C, and E_m is the Kraus operator defined by

$$E_m = {}_C\langle m|\,(U_{T,A\to C,D}\otimes I_B)\,|\mathrm{EPR}\rangle_{A,B}\,. \tag{A2}$$

Here, we note that the state $|m\rangle_C$ is a basis state of the remaining black hole C. We also note that the adjoint HP channel is expressed in terms of the Kraus operators,

$$\mathcal{N}[\mathcal{O}] = \sum_{m=1}^{d_C} E_m^\dagger\mathcal{O}E_m. \tag{A3}$$

Using this Kraus operator, let us investigate the Knill–Laflamme condition [40],

$$P_{\mathrm{code}}E_m^\dagger E_n P_{\mathrm{code}} = \alpha_{mn}P_{\mathrm{code}}\quad\left(\alpha_{mn}=\alpha_{nm}^*\in\mathbb{C}\ \text{with}\ \sum_{m=1}^{d_C}\alpha_{mm}=1\right),\quad \text{for}\ \forall m,n=1,\cdots,d_C, \tag{A4}$$

where P_{code} is a projection operator onto a code subspace in general, but in our setup, P_{code} is assumed to be just given by the identity operator $P_{\mathrm{code}}=I_T$, since all input states should be recoverable under the HP setup. If this condition holds, we can construct a recovery map.[23]

Under Haar random averaging, we can easily evaluate the Knill–Laflamme condition from the expression in Eq. (A2) and Haar average (18),

$$\overline{E_m^\dagger E_n} = \frac{1}{d_C}\delta_{mn}I_T. \tag{A5}$$

This result appears to imply that the Knill–Laflamme condition holds *always* under the averaging, but this is not correct. This is because, even if the Knill–Laflamme condition is satisfied, higher moments of the Knill–Laflamme condition, e.g. $\overline{\left|P_{\mathrm{code}}E_m^\dagger E_n P_{\mathrm{code}}\right|^2}$, might not hold due to contributions coming from Weingarten calculus. We can see their contributions by directly evaluating the second moment,[24]

$$\overline{\left|P_{\mathrm{code}}E_m^\dagger E_n P_{\mathrm{code}}\right|^2} \approx \frac{1}{(d_C)^2}\cdot I_T\left[\delta_{mn}+\frac{d_T}{d_D d_B}\right] \tag{A6}$$

where we used the known result (21) with large-d approximation. Thus, when we do not have enough Hawking radiation D, B compared to the diary T, i.e. $d_Dd_B\lesssim d_T$, we cannot ignore the second term, implying the breakdown of the Knill–Laflamme condition. On the other hand,

[23] See, e.g. Sect. 10.3, in particular, theorem 10.1, of Ref. [52] for the review.

[24] See also Ref. [53] for related discussions.

in the opposite limit $d_D d_B \gg d_T$, where we have enough Hawking radiation, we can ignore the second term, and we get the Knill–Laflamme condition. We note that this is consistent with the decoupling condition (3), since the unitarity means the relation

$$\frac{d_T}{d_D d_B} = \frac{1}{d_C} \cdot \left(\frac{d_T}{d_D}\right)^2, \tag{A7}$$

and the factor $(d_T/d_D)^2$ gives an upper bound of the decoupling condition (3).

Next, we construct a recovery map for the HP quantum channel. With the Knill–Laflamme condition in mind, we consider the following map, which is equal to the adjoint HP channel up to the overall factor d_C,

$$\mathcal{R}[\mathcal{O}] \coloneqq d_C \sum_{m=1}^{d_C} E_m^\dagger \mathcal{O} E_m = d_C \mathcal{N}^\dagger[\mathcal{O}]. \tag{A8}$$

Under the Haar random average, this map gives

$$\begin{aligned}
\overline{\mathcal{R}[\mathcal{N}[\rho_T]]} &= d_C \sum_{m,n=1}^{d_C} \overline{E_m^\dagger E_n \rho_T E_n^\dagger E_m} \\
&\approx d_C \sum_{m,n=1}^{d_C} \left[\overline{E_m^\dagger E_n} \rho_T \overline{E_n^\dagger E_m} + \overline{E_m^\dagger \overline{E_n \rho_T E_n^\dagger} E_m} \right] \\
&= d_C \sum_{m,n=1}^{d_C} \frac{1}{(d_C)^2} \left[\delta_{mn} \rho_T + \frac{\mathrm{tr}[\rho_T]}{d_D d_B} I_T \right] \\
&= \rho_T + \left(\frac{d_T}{d_D}\right)^2 \cdot \frac{1}{d_T} I_T,
\end{aligned} \tag{A9}$$

where in the second line, we used the fact that in the large-Hilbert space dimension limit, Weingarten calculus reduces to Wick calculus, and in the final line, we used $\mathrm{tr}\,\rho_T = 1$ and the relation $d_T d_B = d_C d_D$. In the third line, we encountered the Knill–Laflamme condition for the first term (A5), and the second term disturbs the Knill–Laflamme condition. These two terms in the third line correspond to the first and second terms in Eq. (A6), respectively. Thus, under the situation $d_B d_D \gg d_T$ where the Knill–Laflamme condition holds (approximately), we can ignore the second term of the above result, implying that the map in Eq. (A8) works as a recovery map. This is a quantum information theoretic derivation of the Petz-lite. However, we note that the recovery map here is a little bit different from the one (12) up to the overall factor, but the difference almost vanishes when the condition $d_B d_D \gg d_T$ is satisfied.

Finally, we end this appendix by giving the connection between the Petz map and the Petz-lite in terms of the Kraus operator and the Knill–Laflamme condition. Generally, since the coefficients (α_{mn}) are Hermitian, we can diagonalize the Knill–Laflamme condition by some unitary (U_{mn}) as follows [52]:

$$P_{\mathrm{code}} F_m^\dagger F_n P_{\mathrm{code}} = \lambda_m \delta_{mn} P_{\mathrm{code}} \left(\lambda_m \in \mathbb{R}, \text{with} \sum_{m=1}^{d_C} \lambda_m = 1,\ \lambda_m > 0 \right), \text{ for } \forall m, n = 1, \cdots, d_C, \tag{A10}$$

where $F_m = \sum_n U_{mn} E_n$ is the newly defined Kraus operator. Using this Kraus operator, one can define the following map:

$$\mathcal{R}[\mathcal{O}] \coloneqq \sum_{m=1}^{d_C} \frac{1}{\lambda_m} P_{\text{code}} F_m^\dagger \mathcal{O} F_m P_{\text{code}}. \tag{A11}$$

This map can also be expressed in terms of the original quantum channel by introducing some full rank reference state σ as follows [51]:

$$\mathcal{R}[\mathcal{O}] = \sigma^{1/2} \mathcal{N}^\dagger \left[(\mathcal{N}[\sigma])^{-1/2} \, \mathcal{O} \, (\mathcal{N}[\sigma])^{-1/2} \right] \sigma^{1/2}, \tag{A12}$$

and this is exactly the Petz map. In the recovery map (A11), the factor λ_m prevents us from directly giving the adjoint channel $\mathcal{N}^\dagger$, and we need to introduce the curious factors $(\mathcal{N}[\sigma])^{-1/2}$ and $\sigma^{1/2}$. However, for the case where $\lambda_m = 1/d_C$ $(m = 1, \cdots, d_C)$, one can consider the map in Eq. (A8) instead of the above map. As we have seen, the Haar random case with the Knill–Laflamme condition (A5) is certainly this case.

Appendix B. Operator transpose for the EPR state

In this appendix, we derive the relation in Eq. (55) algebraically. We can show the relation directly as follows:

$$\begin{aligned}
&U^T_{C',D'\to B,T'} \left|\text{EPR}\right\rangle_{C,C'} \otimes \left|\text{EPR}\right\rangle_{D,D'} \\
&= \left(I_C \otimes I_D \otimes U^T_{C',D'\to B,T'}\right) \left|\text{EPR}\right\rangle_{C,C'} \otimes \left|\text{EPR}\right\rangle_{D,D'} \\
&= \frac{1}{\sqrt{d_C d_D}} \sum_{\tilde{C}=1}^{d_C} \sum_{\tilde{D}=1}^{d_D} \left|\tilde{C},\, \tilde{D}\right\rangle_{C,D} \otimes \left(U^T_{C',D'\to B,T'} \left|\tilde{C}, \tilde{D}\right\rangle_{C',D'} \right) \\
&= \frac{1}{\sqrt{d_C d_D}} \sum_{\tilde{C}=1}^{d_C} \sum_{\tilde{D}=1}^{d_D} \sum_{\tilde{B}=1}^{d_B} \sum_{\tilde{T}=1}^{d_T} \left|\tilde{C},\, \tilde{D}\right\rangle_{C,D} \otimes \left|\tilde{B}, \tilde{T}\right\rangle_{B,T'} \cdot {}_{B,T'}\!\left\langle \tilde{B}, \tilde{T}\right| U^T_{C',D'\to B,T'} \left|\tilde{C}, \tilde{D}\right\rangle_{C',D'} \\
&= \frac{1}{\sqrt{d_C d_D}} \sum_{\tilde{C}=1}^{d_C} \sum_{\tilde{D}=1}^{d_D} \sum_{\tilde{B}=1}^{d_B} \sum_{\tilde{T}=1}^{d_T} \left|\tilde{C},\, \tilde{D}\right\rangle_{C,D} \otimes \left|\tilde{B}, \tilde{T}\right\rangle_{B,T'} \cdot {}_{C,D}\!\left\langle \tilde{C}, \tilde{D}\right| U_{A,T\to C,D} \left|\tilde{B}, \tilde{T}\right\rangle_{A,T} \\
&= \frac{1}{\sqrt{d_B d_T}} \sum_{\tilde{B}=1}^{d_B} \sum_{\tilde{T}=1}^{d_T} \left(U_{A,T\to C,D} \left|\tilde{B}, \tilde{T}\right\rangle_{A,T} \right) \otimes \left|\tilde{B}, \tilde{T}\right\rangle_{B,T'} \\
&= \left(U_{A,T\to C,D} \otimes I_B \otimes I_{T'}\right) \left|\text{EPR}\right\rangle_{A,B} \otimes \left|\text{EPR}\right\rangle_{T,T'} \\
&= U_{A,T\to C,D} \left|\text{EPR}\right\rangle_{A,B} \otimes \left|\text{EPR}\right\rangle_{T,T'},
\end{aligned} \tag{B1}$$

where in the fifth equality, we used the unitarity condition of the Hilbert-space dimensions $d_T\, d_B = d_C\, d_D$. □

The above relation implies that the left and right diagrams in Fig. B1 are equivalent.

Appendix C. Convention in the SYK HP protocol

In this appendix, we gather some important definitions and conventions that we use in Sect. 4.

Majorana SYK fermions

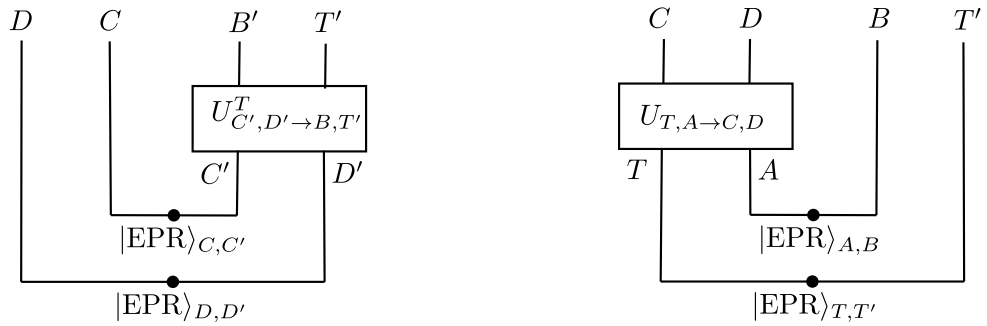

Fig. B1. Diagrams representing the left- and right-hand sides of the relation in Eq. (55). Left: The left-hand side of the relation. Right: The right-hand side of the relation. The left and right diagrams are equivalent.

- Anticommutation relation

$$\left\{\psi_i, \psi_j\right\} = 2\delta_{ij}$$

- The unitary time evolution operator

$$U_\alpha = U_\alpha(t) = \exp\left(itH_\alpha\right) \quad (\alpha = L, R)$$

- Positive direction of time evolutions in left and right SYK systems (in Lorentzian signature)

$$\psi_{i,L}(t) \equiv U_L \psi_{i,L}(0) U_L^\dagger = e^{itH_L}\psi_{i,L}(0)e^{-itH_L},$$
$$\psi_{i,R}(t) \equiv U_R^\dagger \psi_{i,R}(0) U_R = e^{-itH_R}\psi_{i,R}(0)e^{itH_R},$$

  which can be written as

$$\psi_{i,\alpha}(t) = \Delta_L^{-i\frac{t}{\beta}}\psi_{i,\alpha}(0)\Delta_L^{i\frac{t}{\beta}} = \Delta_R^{i\frac{t}{\beta}}\psi_{i,\alpha}(0)\Delta_R^{-i\frac{t}{\beta}} \quad (\alpha = L, R), \tag{C1}$$

  where $\Delta_L = \Delta_R^{-1}$ is the modular operator defined by

$$\Delta_L = \rho_L \otimes \rho_R^{-1} = e^{-K_L} \otimes e^{K_R} = e^{-(K_L - K_R)}, \qquad K_\alpha \equiv \beta H_\alpha \quad (\alpha = L, R). \tag{C2}$$

  Here ρ_α $(\alpha = L, R)$ is defined by

$$\rho_L = \mathrm{tr}_R\left[|\mathrm{TFD}\rangle_{L,R}\langle\mathrm{TFD}|\right], \quad \rho_R = \mathrm{tr}_L\left[|\mathrm{TFD}\rangle_{L,R}\langle\mathrm{TFD}|\right]. \tag{C3}$$

  In the Euclidean signature, one can rewrite the above formal formula as

$$\psi_{i,\alpha}(\tau) = \Delta_L^{\frac{\tau}{\beta}}\psi_{i,\alpha}(0)\Delta_L^{-\frac{\tau}{\beta}} \quad (\alpha = L, R), \tag{C4}$$

  and recover the Lorentzian operator by the analytic continuation $\tau \to -it$.
- Euclidean regularization parametrized by the cutoff δ

$$\psi_{i,L}(t + i\delta) \equiv e^{i(t+i\delta)H_L}\psi_{i,L}(0)e^{-i(t+i\delta)H_L} = e^{(-\delta+it)H_L}\psi_{i,L}(0)e^{(\delta-it)H_L} \tag{C5}$$

  This regularized operator is related to the Euclidean evolved operator (C4) by continuation $\tau \to -it + \delta$.

SYK HP channel

- SYK HP channel (67)

$$\mathcal{N}^{\mathrm{SYK}}_{T\to K,R}[\rho_T] \coloneqq \mathrm{tr}_{\tilde{L}}\left[U_L V_{T,L\to L}\left(\rho_T \otimes |\mathrm{TFD}\rangle_{L,R}\langle\mathrm{TFD}|\right) V^\dagger_{T,L\to L} U_L^\dagger\right]$$

- Adjoint SYK HP channel (68)

$$\mathcal{N}^{\mathrm{SYK}\dagger}_{K,R\to T}[\mathcal{O}_{KR}] \coloneqq \mathrm{tr}_{L,R}\left[|\mathrm{TFD}\rangle_{L,R}\langle\mathrm{TFD}|\left(V^\dagger_{L\to T,L}U^\dagger_L\,\mathcal{O}_{KR}\,U_L V_{L\to T,L}\right)\right]$$
$$= {}_{L,R}\langle\mathrm{TFD}|\left(V^\dagger_{L\to T,L}U^\dagger_L\,\mathcal{O}_{KR}\,U_L V_{L\to T,L}\right)|\mathrm{TFD}\rangle_{L,R}$$

Appendix D. Derivation of correlator from quantum channels

In this appendix, we give the derivation of the relations in Eqs. (86) and (87). We can derive the relation graphically, but below, we give an algebraic derivation of the relation.

We start with the derivation of the relation in Eq. (86), which can be obtained straightforwardly from the definition of the quantum channels in Eqs. (67) and (68). We first note that, from the definition of the quantum channel in Eq. (67), the state $|0\rangle_T\langle 0|$ is mapped to

$$\begin{aligned}\mathcal{N}^{\mathrm{SYK}}_{T\to K,R}[|0\rangle_T\langle 0|] &= \mathrm{tr}_{\tilde{L}}\left[U_L|\mathrm{TFD}\rangle_{L,R}\langle\mathrm{TFD}|U_L^\dagger\right]\\ &= U_R\rho_{KR}U_R^\dagger,\end{aligned} \tag{D1}$$

where we used the fact that $(H_L - H_R)\,|\mathrm{TFD}\rangle_{L,R}$ leads to $U_L\,|\mathrm{TFD}\rangle_{L,R} = U_R\,|\mathrm{TFD}\rangle_{L,R}$, and ρ_{KR} is defined by Eq. (88). For this density matrix, we consider the action of the adjoint channel (68), and take the following matrix element:

$$\left\langle\hat{d}_{\tilde{L}}\right\rangle_\beta \cdot \langle 1|\mathcal{N}^{\mathrm{SYK}\dagger}_{K,R\to T}\left[\mathcal{N}^{\mathrm{SYK}}_{T\to K,R}[|0\rangle_T\langle 0|]\right]|1\rangle = \frac{\left\langle 1\left|\mathcal{N}^{\mathrm{SYK}\dagger}_{K,R\to T}\left[U_R\rho_{KR}U_R^\dagger\right]\right|1\right\rangle}{\mathrm{tr}\left[(\rho_{KR})^2\right]} \tag{D2}$$

where we used the definition in Eq. (73). Using the definition in Eq. (68), we can evaluate the denominator as

$$\begin{aligned}&\langle 1|\mathcal{N}^{\mathrm{SYK}\dagger}_{K,R\to T}\left[\,U_R\,\rho_{KR}\,U_R^\dagger\,\right]|1\rangle\\ &= \left({}_{L,R}\langle\mathrm{TFD}|\otimes{}_T\langle 1|\right)\left(V^\dagger_{L\to T,L}U^\dagger_L\,U_R\,\rho_{KR}\,U_R^\dagger\,U_L V_{L\to T,L}\right)\left(|\mathrm{TFD}\rangle_{L,R}\otimes|1\rangle_T\right)\\ &= \frac{1}{Z_\delta}\cdot{}_{L,R}\langle\mathrm{TFD}|\left(\psi^\dagger_{i,L}(-i\delta)\,U_L^\dagger\,U_R\,\rho_{KR}\,U_R^\dagger\,U_L\,\psi_{i,L}(i\delta)\right)|\mathrm{TFD}\rangle_{L,R}\\ &= \frac{1}{Z_\delta}\cdot{}_{L,R}\langle\mathrm{TFD}|\left(U_R\psi^\dagger_{i,L}(-i\delta)\,U_L^\dagger\,\rho_{KR}\,U_L\,\psi_{i,L}(i\delta)\,U_R^\dagger\right)|\mathrm{TFD}\rangle_{L,R}\\ &= \frac{1}{Z_\delta}\cdot{}_{L,R}\langle\mathrm{TFD}|\left(U_L\psi^\dagger_{i,L}(-i\delta)\,U_L^\dagger\,\rho_{KR}\,U_L\,\psi_{i,L}(i\delta)\,U_R^\dagger\right)|\mathrm{TFD}\rangle_{L,R}\\ &= \frac{1}{Z_\delta}\cdot{}_{L,R}\langle\mathrm{TFD}|\left(\psi^\dagger_{i,L}(t-i\delta)\,\rho_{KR}\,\psi_{i,L}(t+i\delta)\right)|\mathrm{TFD}\rangle_{L,R}\,,\end{aligned} \tag{D3}$$

where in the fourth equality, we used the relation $U_L\,|\mathrm{TFD}\rangle_{L,R} = U_R\,|\mathrm{TFD}\rangle_{L,R}$. Thus, by combining the above expressions, we obtain the relation in Eq. (86),

$$\left\langle\hat{d}_{\tilde{L}}\right\rangle_\beta \cdot \langle 1|\mathcal{N}^{\mathrm{SYK}\dagger}_{K,R\to T}\left[\mathcal{N}^{\mathrm{SYK}}_{T\to K,R}[|0\rangle_T\langle 0|]\right]|1\rangle$$
$$= \frac{1}{Z_\delta}\cdot\frac{\langle\mathrm{TFD}|\psi_{i,L}(t-i\delta)\,\left(I_{\tilde{L}}\otimes\rho_{KR}\right)\,\psi_{i,L}(t+i\delta)|\mathrm{TFD}\rangle}{\mathrm{tr}_{KR}\left[(\rho_{KR})^2\right]}.$$

Next, we derive the relation in Eq. (87). Since $\left\langle \hat{d}_{\tilde{L}} \right\rangle_\beta^{-1} = \mathrm{tr}_{KR}\left[(\rho_{KR})^2\right]$ by the definition in Eq. (73), we focus on the remaining factor $\langle 0|\mathcal{N}^{\mathrm{SYK}\dagger}_{K,R\to T}\left[\mathcal{N}^{\mathrm{SYK}}_{T\to K,R}\left[|0\rangle_T\langle 1|\right]\right]|1\rangle$. To evaluate the factor, we use the definition of the adjoint channel (8),

$$
\begin{aligned}
&\langle 0|\mathcal{N}^{\mathrm{SYK}\dagger}_{K,R\to T}\left[\mathcal{N}^{\mathrm{SYK}}_{T\to K,R}\left[|0\rangle_T\langle 1|\right]\right]|1\rangle \\
&= \mathrm{tr}_{K,R}\left[\mathcal{N}^{\mathrm{SYK}}_{T\to K,R}\left[|0\rangle_T\langle 1|\right]\mathcal{N}^{\mathrm{SYK}}_{T\to K,R}\left[|1\rangle_T\langle 0|\right]\right] \\
&= \mathrm{tr}_{K,R}\left[\mathrm{tr}_{\tilde{L}}\left[U_L|\mathrm{TFD}\rangle_{L,R}\langle\mathrm{TFD}|\psi^\dagger_{i,L}(-i\delta)U_L^\dagger\right]\mathrm{tr}_{\tilde{L}}\left[U_L\psi_{i,L}(i\delta)|\mathrm{TFD}\rangle_{L,R}\langle\mathrm{TFD}|U_L^\dagger\right]\right] \\
&= \mathrm{tr}_{K,R}\left[\mathrm{tr}_{\tilde{L}}\left[U_R|\mathrm{TFD}\rangle_{L,R}\langle\mathrm{TFD}|\psi^\dagger_{i,L}(-i\delta)U_L^\dagger\right]U_RU_R^\dagger\,\mathrm{tr}_{\tilde{L}}\left[U_L\psi_{i,L}(i\delta)|\mathrm{TFD}\rangle_{L,R}\langle\mathrm{TFD}|U_R^\dagger\right]\right] \\
&= \mathrm{tr}_{K,R}\left[U_R\,\mathrm{tr}_{\tilde{L}}\left[|\mathrm{TFD}\rangle_{L,R}\langle\mathrm{TFD}|U_R\psi^\dagger_{i,L}(-i\delta)U_L^\dagger\right]\mathrm{tr}_{\tilde{L}}\left[U_L\psi_{i,L}(i\delta)U_R^\dagger|\mathrm{TFD}\rangle_{L,R}\langle\mathrm{TFD}|\right]U_R^\dagger\right] \\
&= \mathrm{tr}_{K,R}\left[\mathrm{tr}_{\tilde{L}}\left[|\mathrm{TFD}\rangle_{L,R}\langle\mathrm{TFD}|U_L\psi^\dagger_{i,L}(-i\delta)U_L^\dagger\right]\mathrm{tr}_{\tilde{L}}\left[U_L\psi_{i,L}(i\delta)U_L^\dagger|\mathrm{TFD}\rangle_{L,R}\langle\mathrm{TFD}|\right]\right] \\
&= \mathrm{tr}_{K,R}\left[\mathrm{tr}_{\tilde{L}}\left[|\mathrm{TFD}\rangle_{L,R}\langle\mathrm{TFD}|\psi^\dagger_{i,L}(t-i\delta)\right]\mathrm{tr}_{\tilde{L}}\left[\psi_{i,L}(t+i\delta)|\mathrm{TFD}\rangle_{L,R}\langle\mathrm{TFD}|\right]\right].
\end{aligned}
\tag{D4}
$$

By explicitly introducing bases for the traces, we can rewrite the last expression as follows:

$$
\begin{aligned}
&\mathrm{tr}_{K,R}\left[\mathrm{tr}_{\tilde{L}}\left[|\mathrm{TFD}\rangle_{L,R}\langle\mathrm{TFD}|\ \psi^\dagger_{i,L}(t-i\delta)\right]\ \mathrm{tr}_{\tilde{L}}\left[\psi_{i,L}(t+i\delta)\,|\mathrm{TFD}\rangle_{L,R}\langle\mathrm{TFD}|\right]\right] \\
&= \sum_{\alpha,\alpha'=1}^{d_Kd_R}\sum_{a,a'=1}^{d_{\tilde{L}}}\left({}_{KR}\langle\alpha|\otimes{}_{\tilde{L}}\langle a|\right)\left(|\mathrm{TFD}\rangle_{L,R}\langle\mathrm{TFD}|\ \psi^\dagger_{i,L}(t-i\delta)\right)\left(|\alpha'\rangle_{KR}\otimes|a\rangle_{\tilde{L}}\right) \\
&\quad\times\left({}_{KR}\langle\alpha'|\otimes{}_{\tilde{L}}\langle a'|\right)\left(\psi_{i,L}(t+i\delta)\,|\mathrm{TFD}\rangle_{L,R}\langle\mathrm{TFD}|\right)\left(|\alpha\rangle_{KR}\otimes|a'\rangle_{\tilde{L}}\right) \\
&= \sum_{\alpha,\alpha'=1}^{d_Kd_R}\sum_{a,a'=1}^{d_{\tilde{L}}}{}_{L,R}\langle\mathrm{TFD}|\,\psi^\dagger_{i,L}(t-i\delta)\left(|\alpha'\rangle_{KR}\otimes|a\rangle_{\tilde{L}}\right) \\
&\quad\times\left({}_{KR}\langle\alpha|\otimes{}_{\tilde{L}}\langle a|\right)|\mathrm{TFD}\rangle_{L,R}\langle\mathrm{TFD}|\left(|\alpha\rangle_{KR}\otimes|a'\rangle_{\tilde{L}}\right) \\
&\quad\times\left({}_{KR}\langle\alpha'|\otimes{}_{\tilde{L}}\langle a'|\right)\psi_{i,L}(t+i\delta)\,|\mathrm{TFD}\rangle_{L,R} \\
&= {}_{L,R}\langle\mathrm{TFD}|\,\psi^\dagger_{i,L}(t-i\delta)\left(\mathrm{tr}_{KR}\left[|\mathrm{TFD}\rangle_{L,R}\langle\mathrm{TFD}|\right]\otimes I_{KR}\right)\psi_{i,L}(t+i\delta)\,|\mathrm{TFD}\rangle_{L,R} \\
&= {}_{L,R}\langle\mathrm{TFD}|\,\psi^\dagger_{i,L}(t-i\delta)\left(\rho_{\tilde{L}}\otimes I_{KR}\right)\psi_{i,L}(t+i\delta)\,|\mathrm{TFD}\rangle_{L,R}\,,
\end{aligned}
\tag{D5}
$$

where d_K, d_R, $d_{\tilde{L}}$ are the Hilbert-space dimensions of subsystems K, R, $\tilde{L}$, respectively.

Therefore, we get the relation in Eq. (87),

$$
\begin{aligned}
&\left\langle \hat{d}_{\tilde{L}}\right\rangle_\beta\cdot\ \langle 0|\mathcal{N}^{\mathrm{SYK}\dagger}_{K,R\to T}\left[\mathcal{N}^{\mathrm{SYK}}_{T\to K,R}[|0\rangle_T\langle 1|]\right]|1\rangle \\
&= \frac{1}{Z_\delta}\cdot\frac{\langle\mathrm{TFD}|\psi_{i,L}(t-i\delta)\ \left(\rho_{\tilde{L}}\otimes I_{KR}\right)\ \psi_{i,L}(t+i\delta)|\mathrm{TFD}\rangle}{\mathrm{tr}_{KR}\left[(\rho_{KR})^2\right]}.
\end{aligned}
$$

References

[1] G. Penington, J. High Energy Phys. **09**, 002 (2020) [arXiv:1905.08255[hep-th]] [Search INSPIRE].

[2] A. Almheiri, N. Engelhardt, D. Marolf, and H. Maxfield, J. High Energy Phys. **12**, 063 (2019) [arXiv:1905.08762[hep-th]] [Search INSPIRE].

[3] A. Almheiri, R. Mahajan, J. Maldacena, and Y. Zhao, J. High Energy Phys. **03**, 149 (2020) [arXiv:1908.10996[hep-th]] [Search INSPIRE].

[4] G. Penington, S. H. Shenker, D. Stanford, and Z. Yang, J. High Energy Phys. **03**, 205 (2022) [arXiv:1911.11977[hep-th]] [Search INSPIRE].
[5] A. Almheiri, T. Hartman, J. Maldacena, E. Shaghoulian, and A. Tajdini, J. High Energy Phys. **05**, 013 (2020) [arXiv:1911.12333[hep-th]] [Search INSPIRE].
[6] P. Hayden and J. Preskill, J. High Energy Phys. **09**, 120 (2007) [arXiv:0708.4025[hep-th]] [Search INSPIRE].
[7] E. Verlinde and H. Verlinde, J. High Energy Phys. **10**, 107 (2013) [arXiv:1211.6913[hep-th]] [Sear ch INSPIRE].
[8] K. Papadodimas and S. Raju, J. High Energy Phys. **10**, 212 (2013) [arXiv:1211.6767[hep-th]] [Sear ch INSPIRE].
[9] H. Barnum and E. Knill, J. Math. Phys. **43**, 2097 (2000).
[10] D. Petz, Commun. Math. Phys. **105**, 123 (1986).
[11] M. Ohya and D. Petz, Quantum Entropy and Its Use: Theoretical and Mathematical Physics (Springer, Berlin/Heidelberg, 2004).
[12] B. Yoshida, (2021), [arXiv:2106.15628[quant-ph]] [Search INSPIRE].
[13] B. Yoshida, (2021), [arXiv:2109.08691[quant-ph]] [Search INSPIRE].
[14] V. Chandrasekaran and A. Levine, J. High Energy Phys. **06**, 039 (2022) [arXiv:2203.05058[hep-th]] [Search INSPIRE].
[15] Y. Nakata and M. Tezuka, (2023), [arXiv:2303.02010[cond-mat.str-el]] [Search INSPIRE].
[16] Y. Nakayama, A. Miyata, and T. Ugajin (In preparation).
[17] B. Yoshida and A. Kitaev, (2017), [arXiv:1710.03363[hep-th]] [Search INSPIRE].
[18] B. Schumacher and M. A. Nielsen, Phys. Rev. A **54**, 2629 (1996) [arXiv:quant-ph/9604022] [Sear ch INSPIRE].
[19] M. A. Nielsen and D. Poulin, Phys. Rev. A **75**, 064304 (2007).
[20] D. Petz, Rev. Math. Phys. **15**, 79 (2003) [arXiv:quant-ph/0209053] [Search INSPIRE].
[21] S. Vardhan, J. Kudler-Flam, H. Shapourian, and H. Liu, J. High Energy Phys. **01**, 064 (2023) [arXiv:2112.00020[hep-th]] [Search INSPIRE].
[22] J. Kudler-Flam and P. Rath, J. High Energy Phys. **08**, 189 (2022) [arXiv:2203.11954[hep-th]] [Sear ch INSPIRE].
[23] N. Lashkari, Phys. Rev. Lett. **117**, 041601 (2016) [arXiv:1508.03506[hep-th]] [Search INSPIRE].
[24] J. Kudler-Flam, Phys. Rev. Lett. **126**, 171603 (2021) [arXiv:2102.05053[hep-th]] [Search INSPIRE].
[25] J. Kudler-Flam, V. Narovlansky, and S. Ryu, PRX Quantum **2**, 040340 (2021) [arXiv:2108.00011[hep-th]] [Search INSPIRE].
[26] S. Sachdev and J. Ye, Phys. Rev. Lett. **70**, 3339 (1993) [arXiv:cond-mat/9212030] [Search INSPIR E].
[27] A. Kitaev, A simple model of quantum holography, http://online.kitp.ucsb.edu/online/entangled1 5/kitaev/,http://online.kitp.ucsb.edu/online/entangled15/kitaev2/.
[28] S. Sachdev, Phys. Rev. X **5**, 041025 (2015) [arXiv:1506.05111[hep-th]] [Search INSPIRE].
[29] V. Chandrasekaran, T. Faulkner, and A. Levine, J. High Energy Phys. **08**, 143 (2022) [arXiv:2108.01093[hep-th]] [Search INSPIRE].
[30] X.-L. Qi and A. Streicher, J. High Energy Phys. **08**, 012 (2019) [arXiv:1810.11958[hep-th]] [Search INSPIRE].
[31] J. Maldacena and D. Stanford, Phys. Rev. D **94**, 106002 (2016) [arXiv:1604.07818[hep-th]] [Search INSPIRE].
[32] G. Sárosi, PoS **Modave2017**, 001 (2018) [arXiv:1711.08482[hep-th]] [Search INSPIRE].
[33] J. Polchinski and V. Rosenhaus, J. High Energy Phys. **04**, 001 (2016) [arXiv:1601.06768[hep-th]] [Search INSPIRE].
[34] D. Bagrets, A. Altland, and A. Kamenev, Nucl. Phys. B **921**, 727 (2017) [arXiv:1702.08902[cond-mat.str-el]] [Search INSPIRE].
[35] D. J. Gross and V. Rosenhaus, J. High Energy Phys. **12**, 148 (2017) [arXiv:1710.08113[hep-th]] [Se arch INSPIRE].
[36] A. Kitaev and S. J. Suh, J. High Energy Phys. **05**, 183 (2018) [arXiv:1711.08467[hep-th]] [Search IN SPIRE].
[37] A. Romero-Bermúdez, K. Schalm, and V. Scopelliti, J. High Energy Phys. **07**, 107 (2019) [arXiv:1903.09595[hep-th]] [Search INSPIRE].
[38] D. A. Trunin, Usp. Fiz. Nauk **191**, 225 (2021) [arXiv:2002.12187[hep-th]] [Search INSPIRE].

[39] Y. Sekino and L. Susskind, J. High Energy Phys. **10**, 065 (2008) [arXiv:0808.2096[hep-th]] [Search INSPIRE].
[40] E. Knill and R. Laflamme, Phys. Rev. Lett. **84**, 2525 (2000) [arXiv:quant-ph/9604034] [Search IN SPIRE].
[41] P. Gao and D. L. Jafferis, J. High Energy Phys. **07**, 097 (2021) [arXiv:1911.07416[hep-th]] [Search INSPIRE].
[42] A. R. Brown, H. Gharibyan, S. Leichenauer, H. W. Lin, S. Nezami, G. Salton, L. Susskind, B. Swingle, and M. Walter, PRX Quantum **4**, 010320 (2023) [arXiv:1911.06314[quant-ph]] [Search INSPIRE].
[43] T. Schuster, B. Kobrin, P. Gao, I. Cong, E. T. Khabiboulline, N. M. Linke, M. D. Lukin, C. Monroe, B. Yoshida, and N. Y. Yao, Phys. Rev. X **12**, 031013 (2022) [arXiv:2102.00010[quant-ph]] [Search INSPIRE].
[44] S. Nezami, H. W. Lin, A. R. Brown, H. Gharibyan, S. Leichenauer, G. Salton, L. Susskind, B. Swingle, and M. Walter, PRX Quantum **4**, 010321 (2023) [arXiv:2102.01064[quant-ph]] [Search INSPIRE].
[45] F. Pastawski and J. Preskill, Phys. Rev. X **7**, 021022 (2017) [arXiv:1612.00017[quant-ph]] [Search INSPIRE].
[46] G. Bentsen, P. Nguyen, and B. Swingle, (2023), [arXiv:2310.07770[quant-ph]] [Search INSPIRE].
[47] A. M. García-García, B. Loureiro, A. Romero-Bermúdez, and M. Tezuka, Phys. Rev. Lett. **120**, 241603 (2018) [arXiv:1707.02197[hep-th]] [Search INSPIRE].
[48] C. Akers, N. Engelhardt, D. Harlow, G. Penington, and S. Vardhan, (2022), [arXiv:2207.06536[hep-th]] [Search INSPIRE].
[49] M. Berkooz, M. Isachenkov, V. Narovlansky, and G. Torrents, J. High Energy Phys. **03**, 079 (2019) [arXiv:1811.02584[hep-th]] [Search INSPIRE].
[50] H. W. Lin and D. Stanford, SciPost Phys. **15**, 234 (2023) [arXiv:2307.15725[hep-th]] [Search INSP IRE].
[51] H. Barnum and E. Knill, Reversing quantum dynamics with near-optimal quantum and classical fidelity (2000), [arXiv:quant-ph/0004088] [Search INSPIRE].
[52] M. A. Nielsen and I. L. Chuang, Quantum Computation and Quantum Information: 10th Anniversary Edition (Cambridge University Press, New York, 2010).
[53] J. Liu, Phys. Rev. Res. **2**, 043164 (2020) [arXiv:2003.11425[quant-ph]] [Search INSPIRE].

Funded by SCOAP[3].